Report No. FHWA-RD-77-9

STRESS CORROSION SUSCEPTIBILITY OF HIGHWAY BRIDGE CONSTRUCTION STEELS

Phase IIB

October 1976

Final Report

Prepared for

FEDERAL HIGHWAY ADMINISTRATION

Offices of Research & Development

Washington, D. C. 20590

NOTICES

FHWA DISTRIBUTION NOTICE

Sufficient copies of this report are being distributed by FHWA Bulletin to provide a minimum of two copies to each regional office, one copy to each division office, and two copies to each State highway agency. Direct distribution is being made to the division offices.

TECHNICAL REPORT STANDARD TITLE PAGE

1. Report No.	2. Government Accession No.	3. Recipient's Catalog No.
FHWA-RD-77-9		PB272493

4. Title and Subtitle	5. Report Date
STRESS CORROSION SUSCEPTIBILITY OF HIGHWAY BRIDGE CONSTRUCTION STEELS-PHASE IIB	October 1976
	6. Performing Organization Code
7. Author(s)	8. Performing Organization Report No.
R. G. Caton, J. L. Guthrie, C. S. Carter	D6-60217-2
9. Performing Organization Name and Address	10. Work Unit No.
Boeing Commercial Airplane Company P.O. Box 3707 Seattle, Washington 98124	FCP 35F2022
	11. Contract or Grant No.
	DOT FH 11 8280
	13. Type of Report and Period Covered
12. Sponsoring Agency Name and Address	Final Report 31 December 1973 31 October 1976
Federal Highway Administration Office of Research Washington, D.C. 20590	14. Sponsoring Agency Code
	S0641

15. Supplementary Notes

FHWA Contract Manager: H. R. Bosch (HRS-11)

16. Abstract

Eleven steels typically used in highway bridge construction were evaluated for stress corrosion resistance in various environments. The effects of welding and 5% cold work were also investigated. Laboratory tests were verified by exposure of specimens at selected locations in the United States. Both ASTM A325 and ASTM A490 bolts were evaluated for stress corrosion resistance in similar environments. The effects of hot dip galvanizing and mechanical galvanizing on the stress corrosion susceptibility were also determined. Tests were performed in tension.

Suspension cable and prestressing wires were evaluated for stress corrosion resistance. The suspension cable wires were tested with no coating, and with hot dip galvanized and electrogalvanized coatings. Tests were performed in tension.

Corrosion products from the Carquinez Straits bridge were analyzed for chemical composition.

17. Key Words	18. Distribution Statement
Steel Stress corrosion Suspension cable Prestressing wire Bolts	No restrictions. This document is available to the public through the National Technical Information Service, Springfield, Virginia 22161.

19. Security Classif. (of this report)	20. Security Classif. (of this page)	21. No. of Pages	22. Price
Unclassified	Unclassified		PC-A04 MF-A01

Form DOT F 1700.7 (8-69)

CONTENTS

		Page
1.0	INTRODUCTION	1
2.0	MATERIALS	3
	2.1 Structural Steels	3
	2.2 Bolts	4
	2.3 Wires	4
3.0	EXPERIMENTAL PROCEDURE	6
	3.1 Structural Steel Stress Corrosion Test	6
	3.1.1 Specimen Configuration	6
	3.1.2 Specimen Loading	8
	3.1.3 Selection of Initial Stress Intensity Levels	8
	3.1.4 Laboratory Exposures	9
	3.1.5 Field Exposures	9
	3.1.6 Postfracture Examination	10
	3.2 Bolt Stress Corrosion Tests	11
	3.3 Wire Stress Corrosion Tests	12
	3.4 Test Solutions	12
4.0	RESULTS	14
	4.1 Structural Steels	14
	4.1.1 Specimen Loading	14
	4.1.2 Carquinez Bridge Corrosion Product Analysis	14
	4.1.3 Laboratory Exposures	15
	4.1.4 Field Exposure	16
	4.1.5 Microstructural Analysis	16
	4.1.6 Fractographic Analysis	17
	4.2 Bolts	18
	4.3 Wires	18
5.0	DISCUSSION	20
6.0	CONCLUSIONS	22
	REFERENCES	67

FIGURES

No.		Page
1	Eyebar U16N Specimen Location and Orientation	25
2	Eyebar U14N and U14S Specimen Location and Orientation	26
3	Fatigue-Precracked Double Cantilever Beam Specimen Used for Stress Corrosion Testing of Structural Steels	26
4	Sketch of Double Cantilever Beam Specimens Showing Dimensions for Various Specimens	27
5	Method of Loading Double Cantilever Beam Specimens and Measuring Displacement	28
6	Method of Distributing Aqueous Solution from Central Holding Tank to DCB Specimens	28
7	Closeup Showing Method of Controlling Flow Rate with with Hose Clamps and Glass Pipettes	29
8	Specimens Placed at Snohomish River Bridge	29
9	Sulfide Pulp Mill as Seen from Specimen Location at Snohomish River Bridge	30
10	Specimens Placed on South Float of Hood Canal Floating Bridge	30
11	Specimen Location on North Side of Huey P. Long Memorial Bridge	31
12	Specimens Placed on Silver Memorial Bridge	31
13	Specimens Placed at Franklin Institute Science Museum	32
14	Specimens Placed on West Carquinez Bridge	32
15	Bolt Stress Corrosion Test Setup	33
16	Wire Specimen Notch Configuration	33
17	3/16-In.-Diameter Wire Specimens Mounted in Test Fixtures with Attached Extensometer	34
18	Outdoor Facility for Sulfur Dioxide and Hydrogen Sulfide Testing Showing Overlapping Board Construction	34
19	Corrosion Products Taken From West Carquinez Bridge, West Truss	35
20	Corrosion Products Taken From West Carquinez Bridge, East Truss	35
21	Typical Microstructure of 1035 Steel Taken From West Carquinez Bridge Eyebars	36
22	Typical Microstructure of Water Quenched A514 Type F Steel	36
23	Micrographs of Sress Corrosion Cracking in Steels Exposed to 5% Calcium Nitrate/0.25% Ammonium Nitrate Solution	37
24	Crack Branching in Water Quenched A514 Type F Steel Exposed to 5% Calcium Nitrate/0.25% Ammonium Nitrate Solution	39
25	Stress Corrosion Cracking in Steels Exposed to 5% Calcium Nitrate/0.25% Ammonium Nitrate Solution	40
26	Stress Corrosion Cracking in A517 Grade H Steel Exposed to 3.5% Sodium Chloride/0.5% Acetic Acid/Saturated H_2S Solution	41
27	Failed Bolts Exposed to 3.5% Sodium Chloride/0.5% Acetic Acid Saturated with H_2S	41
28	Micrograph from Section of ASTM 490 Bolt Showing Intergrannular Secondary Cracking	42
29	Time to Failure for Bare Prestressing Wire Exposed to 5% Calcium Nitrate/0.25% Ammonium Nitrate Solution	42
30	Typical Cold Worked Microstructure of Prestressing Wire	43

TABLES

No.		Page
1	Steels Recommended for Testing from Phase I	44
2	Chemical Composition and Thickness of Structural Steels Tested in Phases IIA and IIB	45
3	Tensile Properties of Structural Steel	47
4	Chemical Composition of Typical Bolts	48
5	Tensile Properties of A325 and A490 Bolts	48
6	Chemical Composition of Wire Materials	49
7	Wire Tensile Properties Before and After Straightening	49
8	Specimen Identification	50
9	Field Test Sites	51
10	Analysis of West Carquinez Bridge Corrosion Product Samples	52
11	Industries Within an Approximate 5 Mile Radius of Carquinez Bridge	52
12	Results of DCB Stress Corrosion Test in Sulfur Dioxide	53
13	Results of DCB Stress Corrosion Test in Hydrogen Sulfide	54
14	Results of DCB Stress Corrosion Test in Calcium Nitrate and Ammonium Nitrate	55
15	Results of DCB Stress Corrosion Test in 3.5% Sodium Chloride Aqueous Solution	56
16	Results of DCB Stress Corrosion Test in 0.26% Calcium Sulfate Aqueous Solution	57
17	Summary of Alloys Susceptible to Stress Corrosion	57
18	Description of DCB Specimens Remaining at Test Sites	58
19	Results of Field Testing Double Cantilever Beam Stress Corrosion Specimens	59
20	Results of Bolt Stress Corrosion Test in Sulfur Dioxide	60
21	Results of Bolt Stress Corrosion Test in Hydrogen Sulfide	61
22	Results of Bolt Stress Corrosion Test in Calcium Nitrate/Ammonium Nitrate Solutions	62
23	Results of Bolt Stress Corrosion Test in 3.5% Sodium Chloride Solution	63
24	Results of Wire Stress Corrosion Test in 50 ppm Sulfur Dioxide Aqueous Solution	64
25	Results of Wire Stress Corrosion Test in 5 ppm Hydrogen Sulfide Aqueous Solution	65
26	Results of Wire Stress Corrosion Test in 5% Calcium Nitrate/0.25% Ammonium Nitrate Aqueous Solution	66

METRIC CONVERSION FACTORS

Approximate Conversions to Metric Measures

Symbol	When You Know	Multiply by	To Find	Symbol
		LENGTH		
in	inches	*2.5	centimeters	cm
ft	feet	30	centimeters	cm
yd	yards	0.9	meters	m
mi	miles	1.6	kilometers	km
		AREA		
in^2	square inches	6.5	square centimeters	cm^2
ft^2	square feet	0.09	square meters	m^2
yd^2	square yards	0.8	square meters	m^2
mi^2	square miles	2.6	square kilometers	km^2
	acres	0.4	hectares	ha
		MASS (weight)		
oz	ounces	28	grams	g
lb	pounds	0.45	kilograms	kg
	short tons (2000 lb)	0.9	tonnes	t
		VOLUME		
tsp	teaspoons	5	milliliters	ml
Tbsp	tablespoons	15	milliliters	ml
fl oz	fluid ounces	30	milliliters	ml
c	cups	0.24	liters	l
pt	pints	0.47	liters	l
qt	quarts	0.95	liters	l
gal	gallons	3.8	liters	l
ft^3	cubic feet	0.03	cubic meters	m^3
yd^3	cubic yards	0.76	cubic meters	m^3
		TEMPERATURE (exact)		
°F	Fahrenheit temperature	5/9 (after subtracting 32)	Celsius temperature	°C

*1 in = 2.54 (exactly). For other exact conversions and more detailed tables, see NBS Misc. Publ. 286, Units of Weights and Measures, Price $2.25, SD Catalog No. C13.10:286.

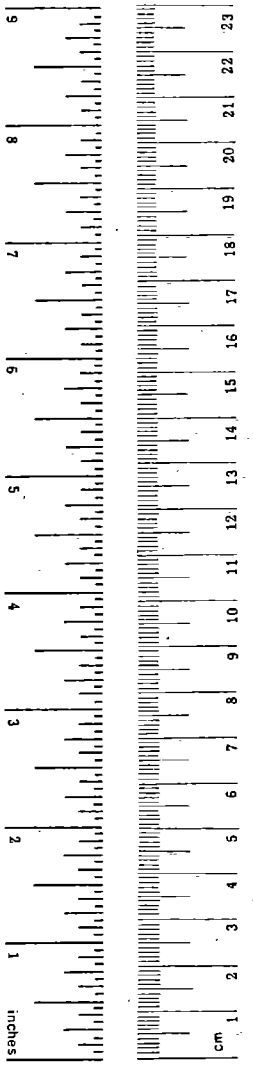

Approximate Conversions from Metric Measures

Symbol	When You Know	Multiply by	To Find	Symbol
		LENGTH		
mm	millimeters	0.04	inches	in
cm	centimeters	0.4	inches	in
m	meters	3.3	feet	ft
m	meters	1.1	yards	yd
km	kilometers	0.6	miles	mi
		AREA		
cm^2	square centimeters	0.16	square inches	in^2
m^2	square meters	1.2	square yards	yd^2
km^2	square kilometers	0.4	square miles	mi^2
ha	hectares (10,000 m^2)	2.5	acres	
		MASS (weight)		
g	grams	0.035	ounces	oz
kg	kilograms	2.2	pounds	lb
t	tonnes (1000 kg)	1.1	short tons	
		VOLUME		
ml	milliliters	0.03	fluid ounces	fl oz
l	liters	2.1	pints	pt
l	liters	1.06	quarts	qt
l	liters	0.26	gallons	gal
m^3	cubic meters	35	cubic feet	ft^3
m^3	cubic meters	1.3	cubic yards	yd^3
		TEMPERATURE (exact)		
°C	Celsius temperature	9/5 (then add 32)	Fahrenheit temperature	°F

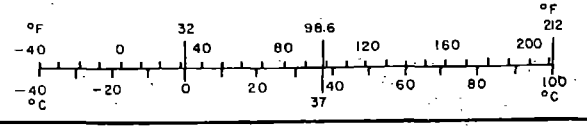

1.0 INTRODUCTION

On December 15, 1967, the Point Pleasant highway bridge collapsed. After an exhaustive investigation, it was concluded that stress corrosion cracking of an eyebar was primarily responsible for the collapse (ref. 1).

The realization that this type of failure could occur in bridge members has focused attention on the fact that stress corrosion has not been a design consideration. Accordingly, the goal of this program was to determine the extent and severity of the potential danger of stress corrosion to highway bridge structures.

Stress corrosion cracking can be defined as cracking due to the combined action of a sustained static tensile stress and a specific environment. A steel may be susceptible to cracking in several different environments.

For cracking to occur during service, certain conditions must exist. The steel must be susceptible to cracking in the service environment, and the applied stress must exceed a minimum level. If these conditions are met, then a crack can extend until its size is sufficient to cause failure by purely mechanical fracture.

Thus, to meet the goals of this program, the following had to be established:

- The types of steels used in highway bridge construction and the magnitudes of the stresses imposed during service.
- The stress corrosion susceptibility of these steels.
- The occurrence of corrosives that can promote stress corrosion cracking in the extreme conditions of the highway enviroment.

To obtain this information the program was divided into two phases. The Phase I study reported in reference 2 was directed to the accumulation of information and the identification of the stress corrosion testing required. Phase II was a testing program and consisted of two parts. Phase IIA involved tests in concentrated solutions to provide an initial identification of susceptible steels. Phase IIB was concerned with testing of susceptible steels in environments that corresponded more closely to highway conditions and included field exposure tests. Portions of the Phase IIA testing are reported in reference 3. Reported herein are the results of the Phase IIB testing. Also included are results of Phase IIA tests completed subsequent to the release of the Phase IIA report (ref. 3).

Phase IIB involved the stress corrosion testing of ASTM specification structural steels, ASTM A325 and A490 bolts, and cable wire used for suspension bridge and concrete prestressing cables. The structural steel testing included an investigation of the effects of welding and cold working. In addition to the ASTM structural steels, material from eyebar members of the West Carquinez Bridge located in Northern California was evaluated as part of the Phase IIB study.

Based on the Phase I study, environments selected for Phase IIA testing were:

- Aqueous solution containing 3.5% sodium chloride
- Aqueous solution of 3.5% sodium chloride and 0.5% acetic acid saturated with hydrogen sulfide
- Aqueous solution saturated with sulfur dioxide
- Aqueous solution of 60% calcium nitrate and 3% ammonium nitrate

With the exception of the 3.5% sodium chloride solution, the concentrations of the above solutions were much greater than would be experienced in service. To more closely approximate service conditions, the following dilute solutions were included in the Phase IIB testing:

- Aqueous solution containing 5 ppm hydrogen sulfide.
- Aqueous solution containing 50 ppm sulfur dioxide.
- Aqueous solution of 5% calcium nitrate and 0.25% ammonium nitrate.

Analysis of corrosion product from the Carquinez eyebars indicated the presence of calcium sulfate. Therefore, in addition to the above environments, stress corrosion tests of eyebar material included exposure to aqueous calcium sulfate solution.

Effects of solution stagnation were also evaluated in Phase IIB. The results of total immersion of specimens in a periodically changed solution were compared with the results of specimens exposed to a continuous feed of fresh solution.

2.0 MATERIALS

2.1 STRUCTURAL STEELS

Based on the Phase I findings (ref. 2) and service experience, it was concluded that carbon steels to ASTM specifications A7, A9, A36, and A373, from which the majority of bridges have been fabricated, are immune to stress corrosion. A number of steels, which could not be classified as resistant to stress corrosion cracking with a high level of confidence, were recommended for testing. The sixteen structural steels recommended for testing from Phase I are given in table 1. Ten of these sixteen steels were obtained for testing. Unfortunately, five steels (A242; A572 grade 60, types 1 and 2; A588 grades E and H) could not be procured in the relatively small quantities required for test purposes. Samples of steel made to the obsolete specification A8 could not be obtained. AISI 1035 steel was unavailable, and AISI 1040 was substituted. Steel to ASTM A572 grade 50 type 2 and grade 60 type 4 was evaluated during Phase IIA but was not included in Phase IIB.

The ten steels procured were in plate form. Their thickness, chemical composition, and supplier are shown in table 2. The chemical compositions of the steels were within specification requirements. The thicknesses corresponded closely to the maximum sizes used in service, except for A572 Grade 50, which could only be obtained in 1-in. plate.

Results of tensile tests performed during Phase IIA on specimens from the quarter thickness location are given in table 3. To obtain tensile properties comparable to those reported for AISI 1035 eyebars (ref. 2) the 1040 steel was water quenched from 1550° F and tempered at 1225° F. The microstructure of the structural steels at the quarter thickness location in the longitudinal direction is given in reference 3.

After the initiation of testing of the AISI 1040 steel, AISI 1035 steel specimens from eyebar members of the West Carquinez Bridge were submitted for stress corrosion testing by the Toll Bridge Authority, California Department of Transportation. The West Carquinez Bridge is a 49-year-old cantilever through truss and suspension bridge that carries I-80 traffic between Vallejo and Crockett, California about 25 miles northwest of San Francisco. The eyebar material was provided in the form of twenty-two 1.46-in.-thick double cantilever beam specimens (ref. 4). The configuration of these specimens was the same as that used for the field and laboratory testing described in subsequent sections of this report. Except for a clean-up allowance of approximately 0.02 in. on each surface, the specimen thickness corresponded to the thickness of the eyebar.

Twenty of the specimens were from the eyebar end designated U16N. The orientation of the specimens relative to eyebar end U16N and the specimen numbering scheme are shown in figure 1. The remaining two specimens were obtained form the eyebar ends designated U14N and U14S as shown in figure 2. The chemical compositions of the eyebar materials are given in table 2. The composition of the eyebars approximated the composition of AISI 1035 steel. In the remainder of this report, the Carquinez eyebar

material will be referred to as AISI 1035 steel. Hardness measurements on specimens from the three eyebars ranged from R_B 88 to R_B 92. These values represented the hardness approximately 0.02 in. from the eyebar surface.

2.2 BOLTS

Bolts were included in the testing program to more clearly define the stress corrosion characteristics. High-strength bolts to ASTM specification A490 can be susceptible to cracking, particularly if heat treated to or above the specification hardness limit. Specification A325 bolts are generally believed to be more resistant to stress corrosion. The sizes and coatings on the bolts evaluated were as follows:

Specification	Size	Coatings
A490	3/4-10 UNC by 4.5	Bare Mechanically galvanized
A325	7/8-9 UNC by 4.0	Bare Dip galvanized Mechanically galvanized
A325	1-1/8 UNC by 6.0	Bare Dip galvanized

Bare and dip galvanized bolts and nuts were obtained from Boeing stores and from local suppliers. Bare bolts and nuts supplied by The Boeing Company were mechanically galvanized by the 3M Company, Saint Paul, Minnesota (ref. 5). The chemical compositions of the bolts are given in table 4; their tensile properties in table 5. The compositions of the bolts were within the limits of the applicable specification. Nuts with the same type of coating as the bolt were used to load the bolts.

2.3 WIRES

High-strength cable wire is known to be susceptible to stress corrosion cracking in a number of environments (ref. 2). Testing of cable wires was included to attempt to establish threshold stress levels below which no cracking occurs.

Five different wires were obtained for evaluation. Four of the wires were for suspension bridge cable applications and one was for cable used to prestress concrete. The chemical compositions are shown in table 6. The wire diameters and the types of coatings on the wires were as follows:

Wire type	Coating	Diameter (In.)
Suspension bridge cable	Bare	0.188
	Dip galvanized	0.192
	Electrogalvanized	0.187
	Galvanized	0.108
Concrete prestressing cable	Bare	0.128

The prestressing wire evaluated was from the center strand of a seven-strand cable obtained from a local contractor. The suspension cable wire was supplied by the Federal Highway Administration. Three of the suspension wires were received in the form of approximately 28-in.-diameter coils. The remaining suspension wire was obtained from the seven center strands of a 37-strand cable. The heavy coating of grease on the wire from the 37-strand cable was removed by vapor degreasing. With the exception of the wire from the seven-strand prestressing cable, straightening of the wires was required prior to specimen fabrication. This was done by stretching and introduced 0.5%-1.1% permanent deformation. The tensile properties of the wires before and after straightening are given in table 7.

3.0 EXPERIMENTAL PROCEDURE

3.1 STRUCTURAL STEEL STRESS CORROSION TEST

3.1.1 SPECIMEN CONFIGURATION

A fracture mechanics approach was adopted for the evaluation of the stress corrosion resistance of the structural steels. Several different types of fatigue-precracked specimens suitable for a fracture mechanics approach were considered. Details of the specimen types and experimental techniques have been given in recent publications (refs. 6 and 7). The different specimen types can be classified with respect to the relationship between the stress intensity factor (K_I) and crack extension. Depending on the method of stressing and/or the geometry of the test piece, the stress intensity can be made to increase or decrease, as the crack length increases. When K increases with crack extension, specimens are most commonly stressed under constant load conditions in tension or bending. By loading several specimens to different initial stress intensity values in the test environment, the threshold level below which no crack growth occurs can be established.

When the double cantilever beam (DCB) specimen selected (fig. 3) for this program is stressed under conditions of constant crack opening displacement, the stress intensity (K_I) decreases with crack extension. The crack opening displacement (measured along the line of load application) was maintained during environmental exposure with a wedge as shown in figure 3. The overall result of this procedure is to cause the load to diminish and, consequently, the K_I to decrease as the crack extends under the influence of environment. In this way, the threshold value can be established as the stress intensity at which the crack arrests or, alternatively, as the value at which the crack speed is no greater than a selected rate.

Stress intensities for the DCB specimen shown in figure 3 can be calculated using equation 1 (refs. 8 and 9):

$$K = \frac{\delta\, Eh \left[3h\,(a + 0.6h)^2 + h^3\right]^{1/2}}{4\left[(a + 0.6h)^3 + h^2\, a\right]} \qquad (1)$$

where:

δ = total deflection of the two arms of the DCB specimen at the load point

E = modulus of elasticity (29 000 000 psi)

2h = specimen height

b = specimen thickness

a = crack length measured from load point

The above equation agrees closely with other expressions obtained by analytical and compliance methods (refs. 10 and 11). For equation 1 to be applicable, however, certain conditions must be fulfilled:

- The bending stress in each arm of the DCB must not exceed the tensile yield strength Y
- (W-a) > 2h in order that equation 1 is not influenced by the length W (fig. 3) (ref. 11)
- $h > 1.5 (K/Y)^2$ (ref. 12)
- a/h > 1.0 (ref. 10)

Double cantilever beam (DCB) specimens with the dimensions shown in figure 4 were used. The notch in each specimen was oriented parallel to the rolling direction (expressed as T-L orientation in ASTM D399-72) except in the specimens machined from the Carquinez eyebar material, whose orientations are shown in figures 1 and 2. The smaller specimens were removed from the larger specimens after completion of Phase IIA testing. Machining of specimens removed directly from plate was controlled so as to remove the minimum amount of material from the plate surface. Specimens taken from cold worked or welded plate were tested in the full section thickness. Each DCB specimen was steel stamped with an identification number as given in table 8.

Cold working of the selected steels (A514 type F and A441) was accomplished by straining 2 in. by 1 in. by 24 in. long bars of material 5% in a tensile machine. Double cantilever beam specimens were removed from the cold worked portion of the bars.

To simulate the structure of a weld heat affected zone, 0.6 in. by 2.1 in. by 5.1 in. specimen blanks of A441 and A514 type F steel were water quenched from 1700° F and specimen blanks of A514 type F steel were air cooled from 1700° F. Approximately 0.05 in. of material was removed from each surface of the 0.60-in.-thick specimen blanks following thermal treatment. Alternative methods of obtaining heat affected zone structure for testing were considered and are discussed in the Phase IIA report (ref. 3).

A chevron notch, of the type specified by ASTM E399-72, was used to facilitate the development of a fatigue crack. The specimens were fatigue cycled in a Vibrophore machine at a frequency of 4000 cpm, and a crack was grown until it extended at least 0.05 times the crack length (a) or a minimum of 0.05 in. beyond the chevron. Applied loads were selected so that the fatigue stress intensity did not exceed the lower of either 30 ksi-in.$^{1/2}$ or the applied K for stress corrosion testing during the last 0.05 in. of crack extension. Following fatigue precracking, the specimens were cut transversely to remove the loading holes. This was considered to be necessary because the presence of the open holes could affect the validity of equation 1. Following removal of the holes and insertion of the wedge, the DCB specimen configuration was as shown in figure 3.

Upon completion of fatigue cracking and hole removal, the crack length (a) on the larger specimens was approximately 3 in. The specimen length (W = 10.25 in.) allowed for stress corrosion crack growth over a length of 3 in. before the (W-a) > 2h

requirement was violated. From equation 1 it can be seen that this corresponds to a reduction of 60% in stress intensity relative to the initial stress intensity at the fatigue crack tip. In other words, if the initial stress intensity was 100 ksi-in.$^{1/2}$, the specimen size allowed for a threshold to be determined in the range 100 to 40 ksi-in.$^{1/2}$.

3.1.2 SPECIMEN LOADING

The double cantilever beam specimens were loaded by means of a 10° tapered wedge displacing the beam arms. The wedges were fabricated from 300M steel heat treated to a hardness of Rockwell R_C 52 minimum. No lubricant was used on the wedges. Required amounts of displacement (eq. 1) were obtained by varying the depth of wedge insertion. The top of the wedge was machined normal to the taper, and the top and bottom of the specimen were machined parallel. The wedge was inserted by means of a Tinius Olsen tensile machine using rigid platens which, with the parallelity built into the wedge and test piece, assured even displacement across the specimen. Displacements were measured during loading by means of vernier calipers across the top of the specimen, and measurements were made to the nearest 0.0005 in. The method of loading is shown in figure 5. After loading, the notch plus fatigue crack length were measured to the nearest 0.01 in., and a reference line was scribed to indicate crack length. This provided a convenient method to visually check for crack growth. All cracks were wetted with the relevant corrosive agent at the time of loading.

3.1.3 SELECTION OF INITIAL STRESS INTENSITY LEVELS

Double cantilever beam specimens have been successfully used to evaluate the stress corrosion susceptibility of several materials (ref. 9). However, if the stress intensity is sufficiently high, a stress corrosion crack may branch and/or run out of plane. If this occurs, a threshold cannot be measured. To guard against such an occurrence, specimens of the same steel exposed to the same environment were loaded to different stress intensity levels. In this way the probability of obtaining a nonbranching crack was increased. Furthermore, the specimens that do not exhibit crack growth provide a lower bound in defining the threshold level.

To determine the threshold stress intensity in most steel/environment combinations, two specimens were loaded to the following stress intensity levels. One specimen was loaded to the maximum stress intensity consistent with elastic behavior by limiting the bending stress in each arm of the DCB specimen to a value less than the yield strength. However, plane strain fracture toughness, K_{IC}, rather than the yield strength, was the limiting factor for some steels. The second specimen was loaded to a lower level of stress intensity. This lower level was equal to or less than the maximum stress intensity under which plane strain conditions could be maintained. The stress intensity for plane strain was determined from the following equation:

$$b > 2.5\,(K/Y)^2 \qquad (2)$$

where b is the specimen thickness (fig. 3).

Some modification of the above approach was required for the tests in saturated hydrogen sulfide solution. Sufficient threshold (K_{ITH}) data had been obtained in previous studies (ref. 2) that estimates of the threshold levels for the steels under evaluation could be made. Accordingly, the stress intensity levels for tests in this environment were selected to span the anticipated stress corrosion threshold range.

3.1.4 LABORATORY EXPOSURES

Several methods were used to expose the loaded DCB specimens to aqueous laboratory environments. For the Phase IIA testing, crack tips were exposed to a continuous flow of solution. Aqueous solutions were held in a central tank and fed through a manifold and drawn glass pipettes to the crack tips (figs. 6 and 7). The rate of solution flow, controlled by means of hose clamps, was adjusted to keep the crack tips moist. Excess solution was collected in a tray and periodically drained away. During Phase IIB testing, the manifold and pipette system was not used. Instead, the crack tip was periodically wetted by squirting the notch with a small jet of aqueous solution from a plastic bottle twice each working day.

A third method used was to immerse the DCB specimen in aqueous solution. Specimens were immersed to a depth such that the crack tip was submerged but not the wedge. Only solutions saturated with hydrogen sulfide or sulfur dioxide were used for the immersion type of testing. The baths in which the specimens were immersed were changed twice each week. Plastic buckets were used to contain the baths. This method evaluated the effect of stagnant solutions on the K_{ISCC} of selected steels.

3.1.5 FIELD EXPOSURES

To provide a correlation between laboratory tests and service environments, loaded DCB specimens were exposed at field locations. Duplicate DCB specimens of A36, A514 type E, A514 type F, and A517 grade H steel were placed at each of six field sites. The field sites and the reasons for their selection are given in table 9. In addition to ASTM specification steels, duplicate specimens fabricated from the AISI 1035 eyebar material were exposed at the Carquinez site.

The specimens were loaded by wedge insertion to the maximum stress intensity consistent with elastic behavior by limiting the bending stress in each arm of the DCB specimen to a value less than the yield strength. A frame constructed of wood and threaded rod was then placed around the specimen to protect the wedge during shipment and exposure. After one year of exposure, one of the duplicate specimens at each site was removed and returned to Boeing for examination. The results of this examination are described in section 4.0. The specimens remaining at the test sites are scheduled to be removed after a total of 3 years' exposure by the Federal Highway Administration.

The specimen placement at the Snohomish River bridge, Everett, Washington is shown in figure 8. Two parallel lift span bridges cross the Snohomish River at the test site. The specimens were placed on top of the north tower of the west bridge. A considerable amount of bird droppings was observed near the top of the tower. Specimens are at

present exposed to large quantities of sulfur emissions from a nearby pulp mill (see fig. 9). However, equipment is currently being installed at the pulp mill that will reduce the amount of sulfur emissions. Less than one mile west of the Everett bridge, the Snohomish River enters Puget Sound. North and east of the test site are rural areas.

The specimen placement at the Hood Canal Floating Bridge in the State of Washington is shown in figure 10. The specimens were located 3 to 4 ft above the water on the north side of the south float. The prevailing southerly winds exposed the specimens to a salt spray. Maintenance personnel at the bridge indicated that protection of exposed metal on the concrete floats was a continual problem. In addition to the marine environment, the Hood Canal Bridge was selected as a test site because of a previously reported stress corrosion failure of an anchor cable.

Specimens at the Huey P. Long Memorial Bridge over the Mississippi at Baton Rouge were placed 4 to 5 ft below the roadway in the space formed by the intersection of several bridge members, as shown in figure 11. During wet weather the specimens are exposed to traffic spray. Although the roadway had been salted 7 to 10 years ago, salting is presently forbidden. A railroad track runs down the center of the bridge; highway traffic is carried along each side of the bridge. Immediately adjacent to the bridge is a bauxite aluminum smelter. Downstream from the bridge on the east bank are several oil refineries and petrochemical plants. A cement plant north of the bridge has been closed down. West of the bridge lie farmlands.

The Silver Memorial Bridge, Henderson, West Virginia (bridge number 2765) crosses the Ohio River in a rural area downstream from the concourse of the Ohio and Kanawha Rivers. The specimens were placed on the web (fig. 12) of the uppermost horizontal member at approximately midspan (section U19-U20). This location was approximately 60 ft above the roadway. The Silver Memorial Bridge is just downstream from the site where the Point Pleasant Bridge collapsed in 1967.

In Philadelphia, specimens were placed on the slate roof of the northwest wing of the Franklin Institute Science Museum. The specimen placement at the Franklin Institute is shown in figure 13. A Continuous Air Monitoring Project (CAMP) station is located at the Institute and daily air quality records are available. Relatively high levels of sulfur emissions have been reported in the Philadelphia area (ref. 2).

The specimens at the West Carquinez Bridge (fig. 14) on Interstate 80 near Vallejo, California were placed on a horzontal member 4 to 5 ft below the roadway. The design of the eyebar members on the 49-year-old West Carquinez Bridge is similar to that for the eyebars of the Point Pleasant Bridge which collapsed in 1967. However, whereas the Point Pleasant Bridge eyebars were AISI 1060 steel, the West Carquinez Bridge eyebars are AISI 1035 steel. Extensive amounts of corrosion products have been found at the eyebar pin joints of the West Carquinez Bridge. Samples of this corroion product were submitted for analysis (ref. 13). The results of the analysis are contained in section 4.0.

3.1.6 POSTFRACTURE EXAMINATION

After exposure, the DCB specimens were broken open by wedge loading. To facilitate fracture, the specimens were cooled in liquid nitrogen. The fracture faces were then

examined under low-power magnification for evidence of stress corrosion crack growth. Selected specimens which exhibited evidence of crack growth were examined using fractographic and metallographic techniques to establish the fracture mode.

In addition, the length of the initial crack was measured according to the procedure described in ASTM E399-72T. The initial stress intensity at the tip of the precrack was calculated using the value obtained by this procedure.

3.2 BOLT STRESS CORROSION TESTS

Bolts were loaded by inserting them in fixtures with oversize holes and torquing the nuts. The fixtures and the loaded bolt were then immersed in an aqueous solution as shown by figure 15. The bolts were periodically checked for failure by hand twisting the nuts. To prevent evaporation losses, the tanks in which the bolts were immersed were covered. Except for the saturated H_2S and SO_2 solutions, the solutions were changed once each month. The saturated solutions were changed biweekly.

The load on the bolts was calculated using the equation:

$$P = EA\frac{\Delta L}{L_1}$$

where:

P = load on bolt resulting from torquing

E = modulus of elasticity (29 000 000 psi)

A = cross-sectional areas of bolt shank

ΔL = change of bolt length (fig. 15)

L_1 = length over which ΔL occurs (fig. 15)

This formula did not account for any loads on the threads and the reduced net section area of the threads. Because the loaded thread length was small relative to the shank length, the effect of neglecting the loaded thread length was insignificant.

The nominal bolt diameter was used to determine A for the above equation. The bolt length L was measured before and after torquing to obtain ΔL. A ball micrometer was used to measure L to the nearest 0.0001 in. To seat the ball micrometer, center holes were drilled on each end of the bolt with a number 3 center drill. The length L_1 in which ΔL occurs was measured with a vernier caliper to the nearest 0.001 in.. Length L_1 was measured after the nut had been tightened as tight as could be achieved with a hand held spud wrench. Final torquing was accomplished with an air powered torquing machine. Bolts were torqued to loads greater than the minimum loads required for bolt installation described in AASHTO M164. Prior to immersion in aqueous solution, the bolt and fixture assemblies were vapor degreased.

If no failures were detected after approximately one year of exposure, the bolts were removed from test. Bolts removed from test were torqued to failure with an air powered torquing machine. This method was chosen because if partial stress corrosion cracking had occurred, failure would be expected at this position, reducing the risk of missing any incipient cracking. The fracture faces thus obtained were examined under low-power magnification for evidence of stress corrosion.

3.3 WIRE STRESS CORROSION TESTS

Stress corrosion testing of the wire materials was conducted with notched specimens which were subjected to sustained tensile loads. Figure 16 shows the notch configuration. After machining, the root radius and the notch depth were measured with an optical comparator.

The fixture used to load the specimens is shown in figure 17. Threads were machined on the ends of the 3/16-in.-diameter specimens to secure the ends of the specimen in the fixture with nuts. The smaller diameter wires were secured by swaging fittings on the ends of the specimens. The wires were loaded by tightening the nuts on the threaded rod columns of the fixtures. The applied stress was measured in terms of strain with a 2-in. gage length averaging, linear-differential-transformer, extensometer. The extensometer was attached to the specimen above the plastic cup shown in figure 17. The plastic cups were placed so that the notch was submerged when the cups were filled with solution. The specimens were exposed by filling the cups with dilute 50 ppm SO_2 solution, dilute 5 ppm H_2S solution, and 5% calcium nitrate/0.25% ammonium nitrate solution.

To restrict evaporation losses, plastic lids with slots to accommodate the wires were placed over the plastic cups. Sealant was used to prevent solution from dripping on the threaded or swaged ends of the specimens when the cups were filled.

The specimens were routinely checked for evidence of failure. The H_2S and SO_2 solution levels were maintained by additions of fresh solution. The 5% calcium nitrate/0.25% ammonium nitrate solution level was maintained by adding water. Approximately every 30 days, the cups on all the specimens were emptied, washed out, and filled with fresh solution.

3.4 TEST SOLUTIONS

Aqueous solutions of H_2S and SO_2 were prepared by bubbling H_2S or SO_2 gas from a cylinder through aqueous solution contained in plastic holding tanks. A gas line connected the cylinder and regulators to diffusers in the holding tanks. Inserted in the gas line were gas flow rate indicators and moisture traps to prevent the solution from being drawn back into the cylinder regulators. To prepare the solutions, gas was bubbled through the solutions until saturation was obtained, usually in 3 to 4 hours. The saturation point was easily discernible since the gas passed straight through the solution rather than being dissolved. The tank used to prepare saturated SO_2 solution was filled with demineralized water. The tank used to prepare saturated H_2S solution was filled with 3.5% NaCl and 0.5% acetic acid solution. This latter solution was used to avoid excessive buildup of corrosion products and to accelerate cracking (ref. 2).

At least twice each week the saturated H_2S and SO_2 solutions were replenished and recharged with gas to maintain saturation. Typical pH values of the saturated solutions were 1.6 for the SO_2 solution and 2.3 for the H_2S solution.

Because of the toxic nature of the sulfur dioxide and hydrogen sulfide, the saturated solutions were prepared in a carefully ventilated outdoor facility (fig. 18). This was constructed with overlapping boards having a significant airspace between them. To avoid cross-contamination, a solid dividing wall was placed between the SO_2 and H_2S tests. Windows were provided as a safety feature so that personnel in the facility could be easily observed. In times of atmospheric stagnation, adequate ventilation was obtained with a fan placed at one door and blowing air through the facility to a door at the opposite end (and through the interconnecting door).

A dilute 50 ppm aqueous SO_2 solution was prepared by adding 1 ml of sulfurous acid with an assay of 7.2% SO_2 to 1543 ml of demineralized water. SO_2 is very soluble in water and gaseous SO_2 reacts with liquid water to form a solution of sulfurous acid. Dilute 5 ppm H_2S solution was prepared by adding 1 ml of the saturated H_2S solution to 762 ml of demineralized water.

Sodium chloride solution was 3.5% sodium chloride in demineralized water. The 60% calcium nitrate and 3% ammonium nitrate solution was prepared as 60 gm of $Ca(NO_3)_2$ and 3 gm of NH_4NO_3 made up to 100 ml of water. The $Ca(NO_3)_2$ was added as $Ca(NO_3)_2 \cdot 4H_2O$ and allowance was made for the water of crystallization. The dilute 5% $Ca(NO_3)_2$ and 0.25% NH_4NO_3 solution was prepared by adding 11 parts of demineralized water to one part 60% $Ca(NO_3)_2$ and 3% NH_4NO_3 solution.

All saturated and dilute H_2S and SO_2 solution stress corrosion testing was accomplished in the outdoor facility shown in figure 18. Temperatures in this outdoor facility varied from nighttime minimums of 34° F to daytime maximums of 80° F. Sodium chloride and calcium nitrate testing was conducted indoors at an ambient temperature of 70° F.

4.0 RESULTS

4.1 STRUCTURAL STEELS

4.1.1 SPECIMEN LOADING

The maximum stress intensity selected for initial loading was limited by the fracture toughness (K_{IC}) or the yield strength as discussed in reference 3. Lower values of applied stress intensity were selected so that plane strain conditions (as determined from equation 2) could be maintained.

No tensile property data were available for the material which was thermally treated to simulate weld structures or for the AISI 1035 eyebar material. Estimates of the yield strengths from hardness data and the tensile property data (table 3) were used to select the initial loads. These estimates were as follows:

Steel	Hardness	Estimated yield strength (ksi)
A441 water quenched	R_C 41-43	150
A514 type F, water quenched	R_C 39-41	135
A514 type F, air cooled	R_C 27-29	110
AISI 1035 eyebars	R_B 88-92	50

Loading to a stress intensity of 65 ksi-in$^{1/2}$ was attempted with the AISI 1035 eyebar material. However, crack extension was observed along the side of the specimen before a stress intensity of 65 ksi-in$^{1/2}$ could be reached. This crack extension indicated that the K_{IC} fracture toughness was less than 65 ksi-in$^{1/2}$. After experiencing crack extension with the first several specimens, subsequent specimens were loaded to a stress intensity of approximately 50 ksi-in$^{1/2}$.

4.1.2 CARQUINEZ BRIDGE CORROSION PRODUCT ANALYSIS

Representative portions of the corrosion product samples (figs. 19 and 20) submitted by the California Department of Transportation (ref. 5) were water washed to obtain a water soluble extract. Similarly, solvent extract was obtained by washing with acetone. Detailed results of the analysis on the as-received corrosion product, the water extract, and the solvent extract are given in table 10.

Two compounds were identified in the water extract; these were $CaSO_4 \cdot 1/2\ H_2O$ (plaster-of-paris) and NaCl. Analysis of the solvent extract detected aliphatic hydrocarbon mixed with some aromatic component. The heating process used to dry the water extract is believed to have converted gypsum ($CaSO_4 \cdot 2H_2O$) to plaster-of-paris ($CaSO_4 \cdot 1/2\ H_2O$).

The presence of NaCl in the water extract was not surprising, since the Carquinez Bridge is exposed to the salt air of San Francisco Bay. The reason for the presence of the gypsum, however, was not immediately apparent. Industries in the vicinity of the Carquinez Bridge as reported by the California Department of Transportation (ref. 14) are listed in table 11. The prevailing winds are generally from west to east at the Carquinez site. Detection of $CaSO_4$ prompted the inclusion of stress corrosion testing of AISI 1035 eyebar material in an aqueous environment of 0.26% $CaSO_4 \cdot 2H_2O$. At room temperature the solubility of $CaSO_4 \cdot 2H_2O$ in water is approximately 0.22%.

4.1.3 LABORATORY EXPOSURES

Details of the DCB specimen stress corrosion test results are given in tables 12 through 16. The specimens listed in these tables were exposed as described and then broken open. The fracture faces thus obtained were examined for evidence of crack growth. The final stress intensities listed in these tables were calculated from equation 1 using the crack length measured on the fracture face. When no stress corrosion crack growth was detected, the initial value of stress intensity corresponded to the final value. Under the condition of constant deflection of the specimen beam arms, the stress intensity diminishes when crack growth occurs. The value of stress intensity when crack growth arrests is thus the stress intensity threshold for stress corrosion (K_{ISCC}).

Of the as-received steels tested, the following showed no susceptibility to stress corrosion cracking in any of the test environments.

A36
A441
A514 type F
A572 grade 50
A572 grade 60
A588 grade A
AISI 1040
AISI 1035

Three as-received steels exhibited varying degrees of susceptibility in the 3.5% sodium chloride/0.5% acetic acid saturated hydrogen sulfide solution. These were:

A514 type E
A514 type F
A517 grade H

The results for these steels are summarized in table 17. Interestingly, the K_{ISCC} for A517 grade H in the hydrogen sulfide solution allowed to stagnate was 50% lower than for continuous flow of the saturated hydrogen sulfide solution.

Also summarized in table 17 are the results of the simulated weldments. The fast and slow cooled A441 and A514 type F alloys were only exposed to dilute solutions. Cracking only occurred in the steels exposed to the 5% calcium nitrate/0.25% ammonium nitrate

solution. Thresholds were difficult to define due to out-of-plane crack extension and crack branching. It is interesting to note that cracking occurred in both the slow cooled and water quenched A514 type F specimens. It appears that alloy hardness is not the only requirement for stress corrosion susceptibility. Further comment on this phenomenon is made in section 4.1.5.

4.1.4 FIELD EXPOSURE

The field test sites and specimen placements are described in section 3.0. After one year of exposure, one of each of the duplicate specimens at each location was removed and broken open. The fracture faces thereby obtained were examined for evidence of stress corrosion. The specimens remaining at the field locations are listed in table 18. This table includes the measurement of the DCB specimen arm deflections introduced by wedge loading. When these remaining specimens are broken open after completion of the 3-year exposure and the final crack length measurements obtained, the deflection values can be used to calculate the final stress intensity levels from equation 1. The specimens remaining at the field location are scheduled for removal in August 1978.

When the specimens listed in table 18 were removed from test, inspection indicated that the original specimen placements were intact and undisturbed. During inspection at the Baton Rouge site, specimens AA8, AA7, and BB14, which were located adjacent to the south flange of a vertical member, appeared to be more severely corroded than other specimens at the site. The area adjacent to the south flange receives maximum traffic spray during wet weather.

After the removed specimens had been collected in the laboratory, examination showed that each field site yielded a characteristic form of general corrosion. Specimens from the same field location could be identified by the color and texture of the general corrosion. The different steels from the same location, however, displayed no distinguishable general corrosion characteristics by which the steels could be identified. The specimens exposed to the marine environment at the Hood Canal location were more severely corroded than specimens from the other five field exposure sites.

The specimens removed from the field sites were broken open and the fracture faces examined. None of the fracture faces displayed any crack growth that could be attributed to stress corrosion. The stress intensities calculated using the crack length measurements taken from the fracture faces are listed in table 19.

4.1.5 MICROSTRUCTURAL ANALYSIS

Metallographic studies were performed on selected alloys exhibiting stress corrosion cracking. In addition, the microstructure of the AISI 1035 eyebar material from the West Carquinez Bridge was evaluated. The 1035 steel consisted of a ferrite/carbide aggregate with evidence of moderately well developed carbide precipitation. Eyebars are typically manufactured from a quenched and tempered steel. The 1035 however, in the 1-1/2-in. section size, would not through harden (based on a martensitic reaction), but would probably transform to an intermediate product. In fact, the microstructure does appear to be a fine pearlite which has been highly tempered. A typical view of the microstructure is shown in figure 21.

The A514 type F steel was both air cooled and water quenched to simulate various areas of weldments. Both conditions exhibited tendencies to stress corrosion cracking in the 5% calcium nitrate/0.25% ammonium nitrate solution. The typical structure of the water quenched condition may be seen in figure 22. The structure is typically bainitic in appearance, the alloy not developing enough hardenability to produce a martensitic structure. The air cooled condition of this alloy was typically a ferrite/carbide aggregate, as would be expected. Fairly extensive grain boundary carbides were apparent and stress corrosion cracking had progressed along these grain boundaries.

Figure 23(a) and (b) are typical examples of the microstructure of slow cooled A514 type F and the morphology of stress corrosion cracking seen in this alloy when exposed to the dilute calcium nitrate/ammonium nitrate solution. Figure 23(a) shows a typical intergranular, secondary crack. Figure 23(b) shows intergranular cracking progressing along the carbide-containing grain boundaries. The microstructure of the A441 steel, water quenched, exhibited pro-eutectoid grain boundary ferrite. The structure appeared somewhat acicular in nature suggesting a fine upper bainite as opposed to pearlite. The crack morphology was obscured by the extensive corrosion occurring on the fracture surface. A heavy corrosion product may be seen on the fracture surface in figure 23(c). Examination of a secondary crack revealed the fracture morphology to be intergranular. This may be seen in figure 23(d).

4.1.6 FRACTOGRAPHIC ANALYSIS

Visual examination of exposed stress corrosion fractures showed a heavy corrosion product due to extensive exposure to the environment after cracking had arrested. Figure 24(a) shows specimen FF6, a water quenched A514 type F alloy exposed to the 5% calcium nitrate/0.25% ammonium nitrate solution. The crack branched immediately at the tip of the fatigue crack and progressed by stress corrosion. Figure 24(b) shows the fracture surface of the right leg of the specimen. Stress corrosion has progressed to within 0.21 in. of the specimen edge.

Stress corrosion cracking in the slow cooled A514 type F material is shown in figure 25(a). The stress corrosion crack immediately left the plane of the fatigue crack and no analysis was available to determine K_{ISCC}. The stress corrosion crack was heavily corroded by the 5% calcium nitrate/0.25% ammonium nitrate solution.

Stress corrosion crack morphology of the water quenched A441 was similar to that seen in the A514 type F alloy. In both cases stress corrosion cracking occurred in the 5% calcium nitrate/0.25% ammonium nitrate solution. Figure 25(b) shows the typical crack morphology seen in the A441 alloy.

Exposure to the saturated hydrogen sulfide/3.5% NaCl/0.5% acetic acid solution produced crack morphologies in stress corrosion similar to those seen in the calcium/ammonium nitrate. Figure 26 shows the stress corrosion crack in the A517 grade H steel.

Both scanning electron and transmission electron fractography proved unsuccessful in identifying fracture morphology due to the extensive corrosion of the fracture surfaces. Fracture modes were restricted to identification by metallography. Success of this method was due mainly to the existence of secondary cracks which had suffered minimum corrosion.

Electron microprobe analysis of the fracture surfaces indicated that the corrosion products were an oxide of iron. Some evidence of salts of the corrosive environments was observed, as would be expected (mainly calcium salts and iron sulfide as relevant). Postfracture corrosion probably accounted for the corrosion products observed.

4.2 BOLTS

A total of 90 bolts were stress corrosion tested. Details of the test results are given in tables 20 through 23. Bolts failed only in the aqueous solution of 3.5% NaCl and 0.5% acetic acid saturated with H_2S (of the 14 bolts tested, 10 failed). None of the bolts exposed to the 5 ppm H_2S aqueous solution failed. All failures occurred in less than 1008 hours. Types of failures are shown in figure 27, the most typical being the thread root failure shown in figure 27(c). The concentration of H_2S in the saturated solution was much greater than would be experienced in actual bridge environments (ref. 2). These failures in the saturated H_2S solution (table 21) did not reveal any differences of stress corrosion susceptibility that could be related to the type of coating, bolt size, or ASTM specification. Exposure times in the dilute solutions ranged from a minimum of 7500 hr to a maximum of 11 500 hr.

Metallographic sections through the fracture faces of the failed bolts displayed secondary intergranular cracking as shown by figure 28. The crack morphology on the main fracture was obscured by extensive corrosion. As a result of the metallographic examination it was determined that stress corrosion cracking in the hydrogen sulfide solution was intergranular in nature.

The remaining bolts, which did not fail, were removed from the test environment and torqued until fracture occurred. This procedure revealed no evidence of cracking as a result of exposure to the sulfur dioxide (table 20), calcium nitrate/ammonium nitrate (table 22), or sodium chloride environments (table 23).

During Phase IIA testing (ref. 3), cracking of bolts in both saturated H_2S and saturated SO_2 aqueous solutions was reported, whereas no cracking was detected in the calcium nitrate/ammonium nitrate or sodium chloride environments. Although extensive general corrosion was observed, no cracking was detected with bolts exposed to the saturated SO_2 solution during Phase IIB testing. The reason for this difference between the Phase IIA and IIB results was not immediately apparent.

4.3 WIRES

A total of 60 wire specimens were stress corrosion tested. Details of the test results are given in tables 24 through 26. Notched specimens loaded in tension were exposed to 50 ppm SO_2 aqueous solution (table 24), 5 ppm H_2S aqueous solution (table 25), and 5% $Ca(NO_3)_2$/0.25% NH_4NO_3 solution (table 26). Specimens from a bare (not galvanized)

prestressing wire were loaded to stress levels up to 80% of the tensile ultimate strength. ASSHTO standard specifications for highway bridges limit the maximum stress on prestressing steel to 80% of the ultimate strength. Specimens from suspension bridge cable wire were loaded to approximately 40% of the ultimate strength.

Extensive general corrosion was observed on the bare specimens in the three test environments. While no rust was detected, a white powdery substance believed to be zinc oxide was observed on the surfaces of the galvanized specimens. Failure occurred only in the bare prestressing wire specimens exposed to 5% $Ca(NO_3)_2$/0.25% NH_4NO_3 solution. Of six specimens tested, four failed. Exposure times for these specimens are illustrated by figure 29. Fracture initiated in the roots of the notches, and the fracture faces displayed evidence of longitudinal splitting. This fracture behavior was attributed to the material anisotropy caused by cold working. Examination of the wire microstructure revealed a cold worked structure, as shown in Figure 30.

The prestressing wire tests indicated a susceptibility to stress corrosion in a calcium nitrate/ammonium nitrate environment at stress levels of 150 ksi. This susceptibility is confirmed by service experience. Several failures of prestressing wire in concrete have been attributed to nitrates in the soil (refs. 15 and 16). Although no susceptibility was detected in the 50 ppm SO_2 or 5 ppm H_2S solutions, sulfides have been cited as an environment in which cracking of prestressing wire occurs (ref. 2). Unless failure occurred, exposure times range from 6700 hr to more than 10 000 hr.

5.0 DISCUSSION

On the basis of the laboratory and field testing results it is apparent that stress corrosion of highway bridge steels, in the typical highway environments encountered, is not a major problem. Only three steels showed susceptibility and this was in the saturated hydrogen sulfide solution. When the solution concentration was reduced to 5 ppm hydrogen sulfide, no crack growth was observed. Even this concentration of hydrogen sulfide is many times that occurring naturally and indicates that abnormal conditions would have to prevail to make stress corrosion operate as a cause of crack growth.

However, of particular significance are the results of the steels heat treated to simulate weldments. These were not tested in either of the saturated hydrogen sulfide or sulfur dioxide environments, but only in the dilute solutions. Interestingly, no crack growth was observed in the dilute hydrogen sulfide and sulfur dioxide solutions. However, significant crack growth occurred in the 5% calcium nitrate/0.25% ammonium nitrate solution. No differences in susceptibility to stress corrosion cracking were seen between the rapidly cooled and slow cooled material. These results, coupled with the present increasing use of welding on construction, indicate a possible area of concern in regard to stress corrosion cracking. In-service cracks, dynamic in nature, have been reported occurring associated with welded structure (for example, cover plate welds). The finding that welded material does show an increased susceptibility to stress corrosion cracking may indicate a synergistic effect in regard to crack propagation. That is to say, fatigue cracks initiated in these areas may extend by a combination of fatigue and stress corrosion. Identification of the role of stress corrosion appears to be possible, since based on this study crack propagation has been shown to be intergranular whereas fatigue cracking usually progresses in a transgranular mode.

The effects of cold work were evaluated. No stress corrosion cracking was observed which could be related to cold working of the A441 or A514 type F. This result is encouraging in view of the occurrence of mechanical damage which may be sustained by bridge members. Elimination of stress corrosion as a problem in these instances means that mechanical damage need only be repaired to the extent of reducing the stress concentration effect (for example, smoothing of sharp notches to prevent fatigue crack initiation). Based on this study the remaining cold work in the member after such an operation is not detrimental to stress corrosion cracking resistance.

Bolts manufactured to ASTM A325 do not appear to be susceptible to stress corrosion cracking. The initial results reported in Phase IIA of cracking in saturated sulfur dioxide may have been due to a poorly controlled method of loading the bolts. Cracking due to overloading may well have caused failure in such an acidic solution. This solution causes considerable dissolution of the steel (ref. 3). The results in Phase IIB using more accurate methods of controlling bolt preload did not duplicate the initial results in that no cracking was observed in tests conducted in the sulfur dioxide solution.

ASTM A490 bolts did fail in the saturated hydrogen sulfide solution. However, based on the type of environment typically encountered around highway bridges, stress corrosion of bolts made of this steel is considered not to be a problem.

Suspension cable wires, both galvanized and bare, with notches representing a severe stress concentration, did not show any susceptibility to stress corrosion cracking in the environments to which they were exposed. This may be due to the fairly low level of stress to which they are tensioned (40% of tensile ultimate strength). Interestingly enough, prestressing wire failed in the dilute nitrate solutions at stresses as low as 56% of ultimate. Two points emerge from this study which are considered significant:

1. Suspension cable wire should not be stressed above 40% of tensile ultimate strength (TUS) since prestressing wire, which has the same chemical composition, showed susceptibility to stress corrosion cracking when loaded to 56% TUS. It should be noted that the prestressing wire was higher strength than the suspension cable wire but that straightening of the latter in this study probably increased its strength to a comparable level.

2. Prestressing wire has been reported to have failed from stress corrosion in areas containing nitrate (refs. 15, 16). This has been confirmed in this study, and in view of the fact that prestressing wire is typically stressed to 70% - 80% TUS, care should be taken when using this material in areas suspected of containing nitrates. Lowering the stress, even if practicable, is no guarantee of obviating stress corrosion cracking since failures at stresses as low as 56% TUS were observed, and failure may even occur at lower stresses given enough time. The lowest stress evaluated in this study was the 56% of tensile ultimate strength.

Finally, the corrosion products taken from the west span of the Carquinez Bridge, consisting basically of calcium sulfate, appear to be innocuous in regard to stress corrosion cracking. No crack extension was observed in the laboratory tests in saturated solutions of calcium sulfate nor at the precracked samples exposed at the Carquinez Bridge site. Thus stress corrosion cracking of the Carquinez Bridge steel in the observed environment does not appear to be a problem.

6.0 CONCLUSIONS

Three steels in the as-received condition exhibited measurable stress corrosion thresholds in the 3.5% sodium chloride/0.5% acetic acid/saturated hydrogen sulfide solution. These steels were:

A514 type F (K_{ISCC} = 45 ksi-in$^{1/2}$)

A514 type J (K_{ISCC} = 18 ksi-in$^{1/2}$)

A517 type H (K_{ISCC} = 36 ksi-in$^{1/2}$)

In addition, the A517 grade H steel showed a K_{ISCC} of 24 ksi-in$^{1/2}$ in a stagnant and saturated solution environment.

No stress corrosion susceptibility was detected in the sulfur dioxide, hydrogen sulfide, sodium chloride, or calcium nitrate/ammonium nitrate test environments with the following steels:

A36	A572 grade 60
A441	A588 grade A
A514 type F	AISI 1040
A572 grade 50	AISI 1035

No effect of 5% cold work on the stress corrosion susceptibility of A514F and A441 was observed.

Simulated weldments showed stress corrosion susceptibility in the 5% calcium nitrate/0.25% ammonium nitrate solution. Steels selected for this treatment were:

A441, water quenched (K_{ISCC} = 28 ksi-in$^{1/2}$)

A514 type F, water quenched (K_{ISCC} < 50 ksi-in$^{1/2}$)

A514 type F, air cooled (K_{ISCC} < 79 > 40 ksi-in$^{1/2}$)

Simulated weldments were not tested in the saturated sulfur dioxide or saturated hydrogen sulfide solutions.

Metallographic analyses revealed that stress corrosion crack morphologies were intergranular in the calcium/ammonium nitrate and hydrogen sulfide type solutions. No correlation was observed between hardness and stress corrosion susceptibility in the simulated weldments of A514 type F. Both the soft, slow cooled and the water quenched A514 type F steel exhibited stress corrosion cracking. Stress corrosion cracking in the softer material appeared to be associated with the grain boundary carbides.

Fractographic analyses by means of electron microscopy were unsuccessful due to the extensive corrosion of the crack surfaces. Electron microprobe analyses revealed the corrosion product to be basically an iron oxide, although postfracture corrosion probably influenced the results.

No repetition of the bolt failures reported in Phase IIA in saturated sulfur dioxide solution was obtained. Failures occurred only in the 3.5% sodium chloride/0.5% acetic acid solution saturated with hydrogen sulfide with the following bolts:

ASTM 490 3/4-10 UNC	(bare and mechanically galvanized)
ASTM 325 7/8-9 UNC	(bare and hot dip galvanized)
ASTM 325 1-1/8-7 UNC	(bare and dip galvanized)

Sustained-load, notched-wire specimens were tested in 5 ppm hydrogen sulfide solution, 50 ppm sulfur dioxide solution, and 5% calcium nitrate/0.25% ammonium nitrate solution. No failures were observed with bare and galvanized suspension wires stressed to 40% of the ultimate strength. Pre-stressing wire loaded to stress levels of 80% of the ultimate strength failed only in the dilute calcium nitrate/ammonium nitrate solution. Failures in this solution occurred at stress levels as low as 150 ksi or 56% of the ultimate strength.

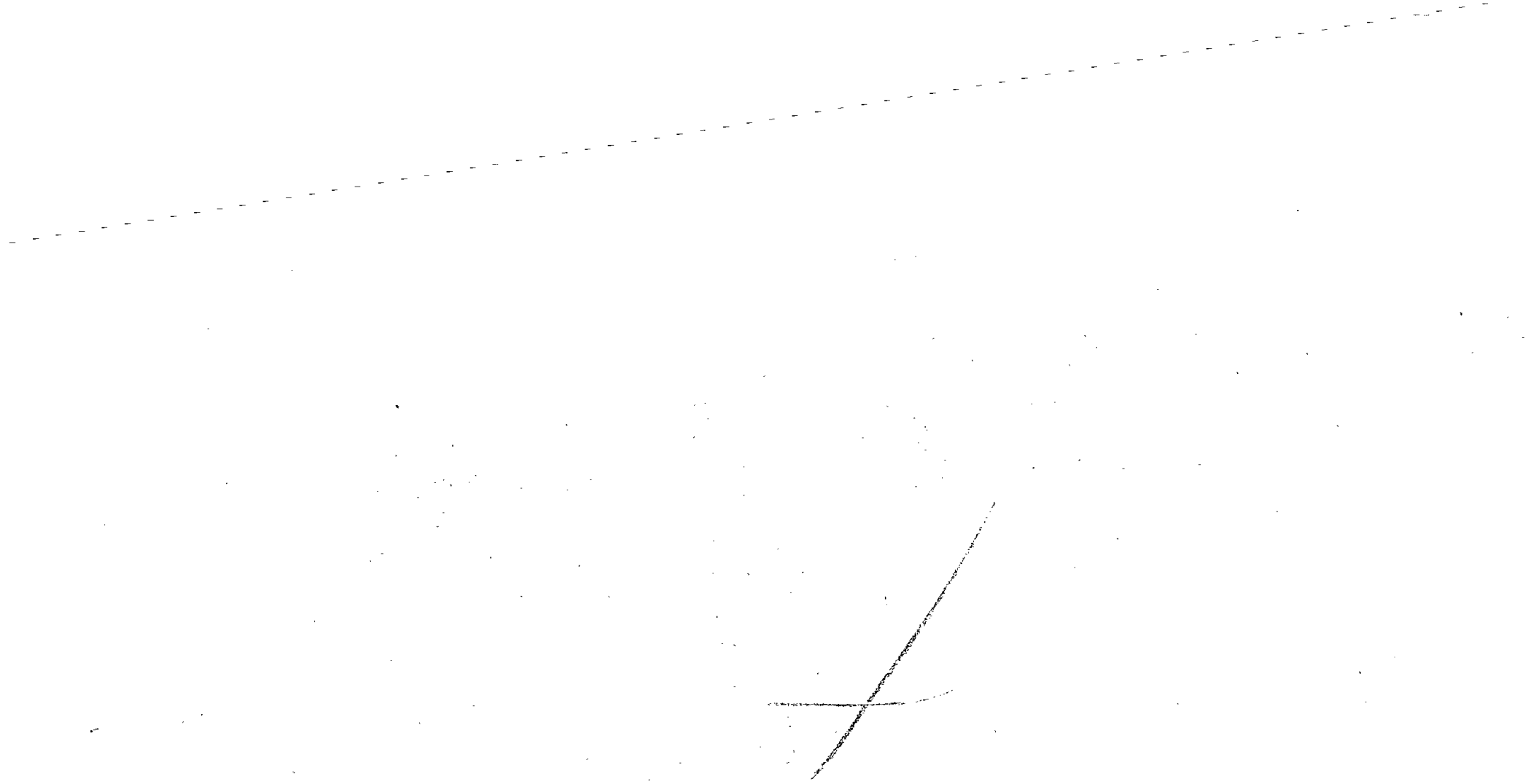

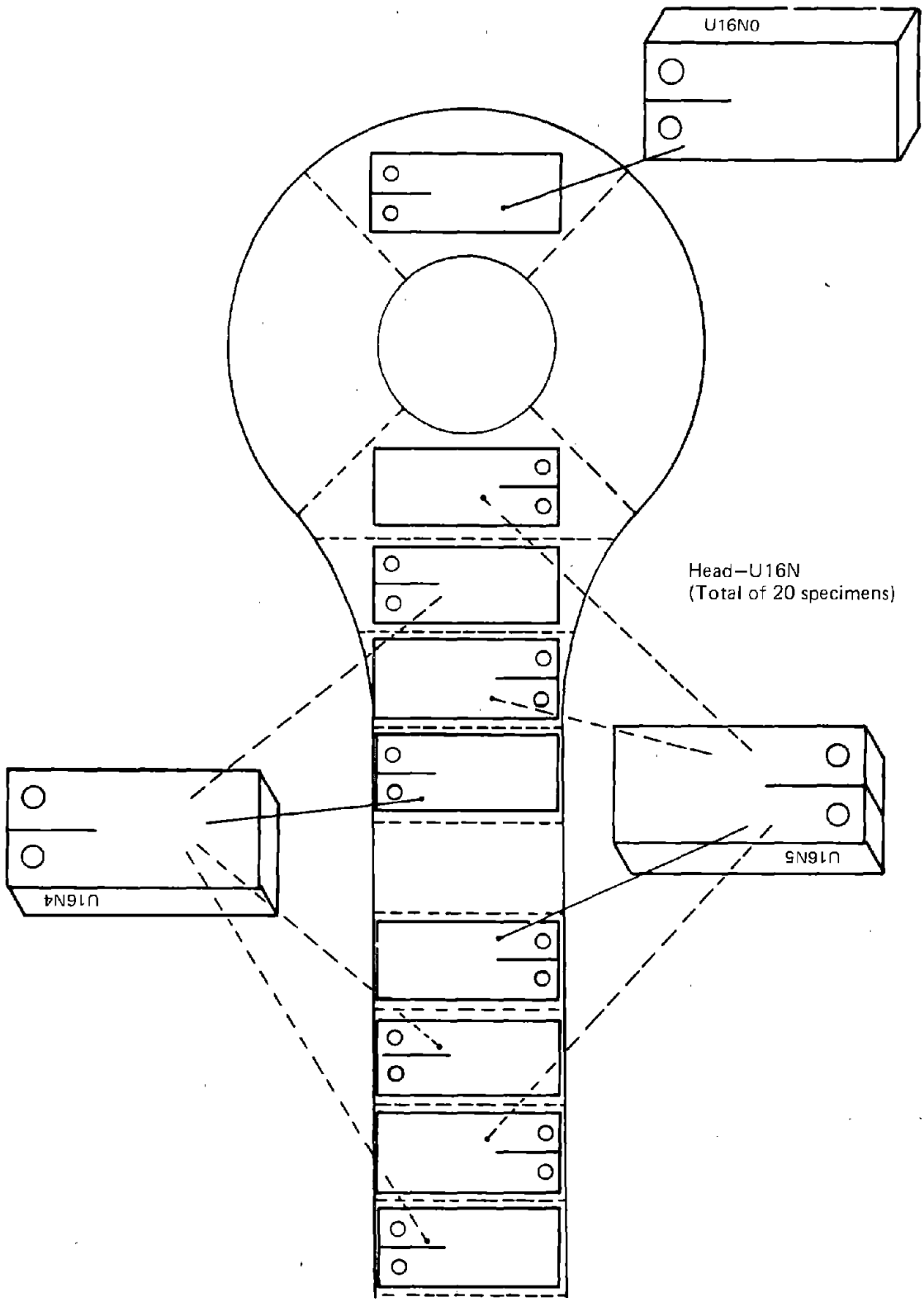

Figure 1.—Eyebar U16N Specimen Location and Orientation (ref. 4)

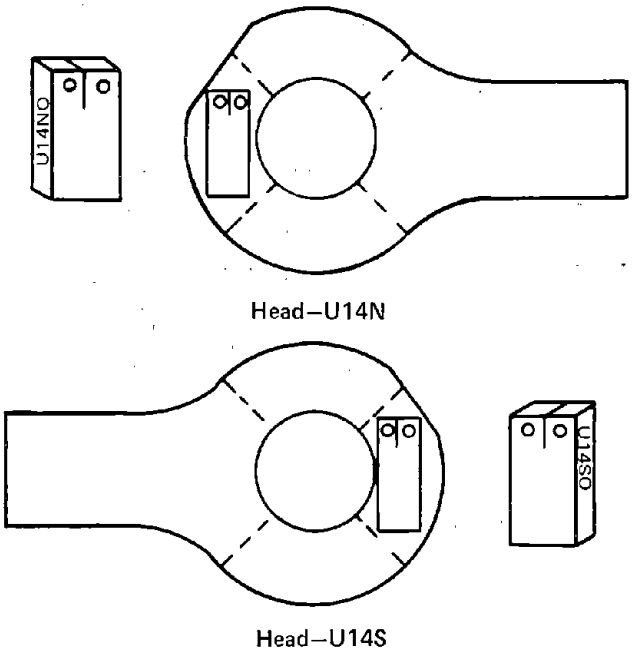

Figure 2.—Eyebar U14N and U14S Specimen Location and Orientation (ref. 4)

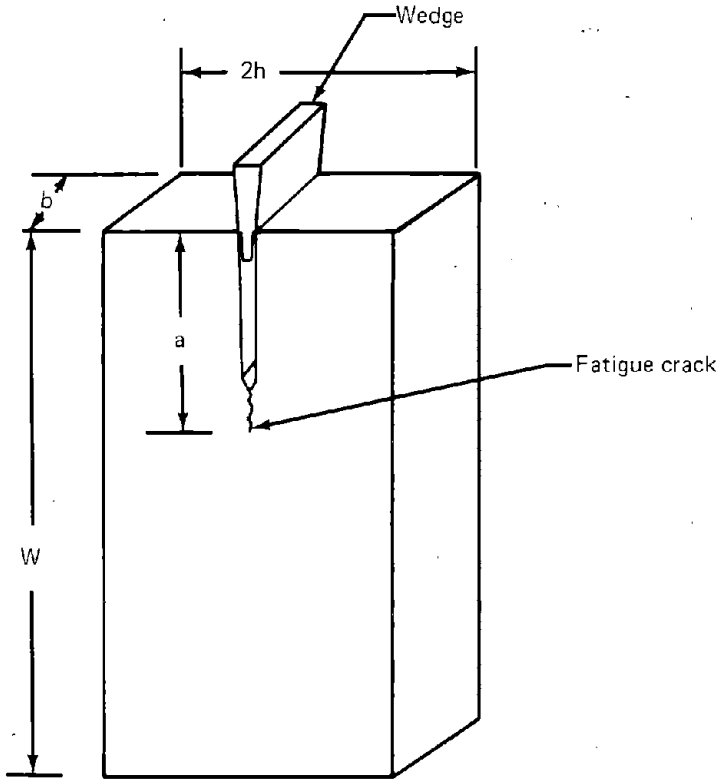

Figure 3.—Fatigue-Precracked Double Cantilever Beam Specimen Used for Stress Corrosion Testing of Structural Steels

Nominal plate thickness	1 2h	2 b	3	4	5	6	7
1¼ in.	4.93 4.90	0.90 0.90	1.00 1.00	4.45 4.45	1.00 1.00	1.20 1.20	11.75 11.90
2¼ in.	4.93	2.15	1.00	4.45	1.00	1.20	11.75
3 in.	4.93 4.90	2.90 0.90	1.00 1.00	4.45 4.45	1.00 1.00	1.20 1.20	11.75 11.90
Cold worked (1 in.)	2.00	1.00	0.50	3.70	0.44	0.45	8.00
Welded (1 in.)	1.84	1.00	0.50	3.70	0.44	0.37	8.00
Removed from broken larger specimens	2.00 2.00	0.75 0.50	0.50 0.50	2.00 2.00	0.50 0.50	0.50 0.50	5.00 5.00

Note: All dimensions are in inches.

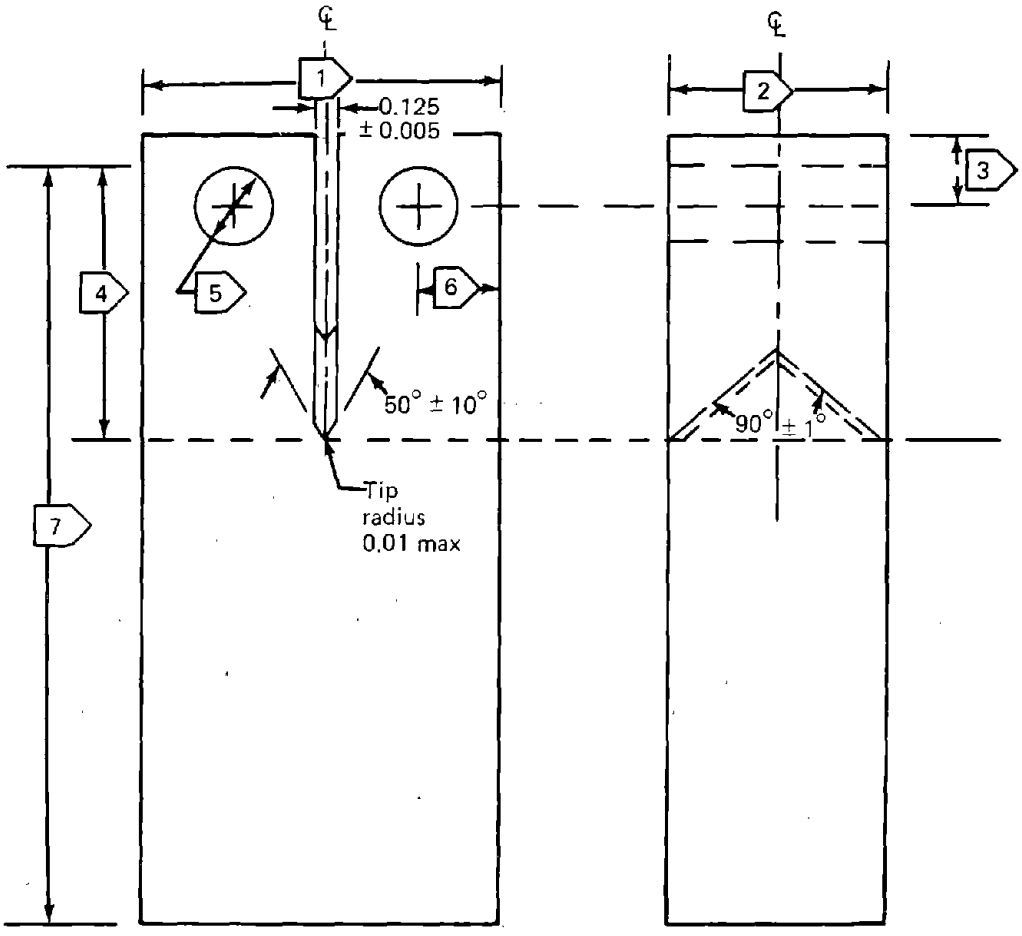

Figure 4.—Sketch of Double Cantilever Beam Specimens Showing Dimensions for Various Specimens

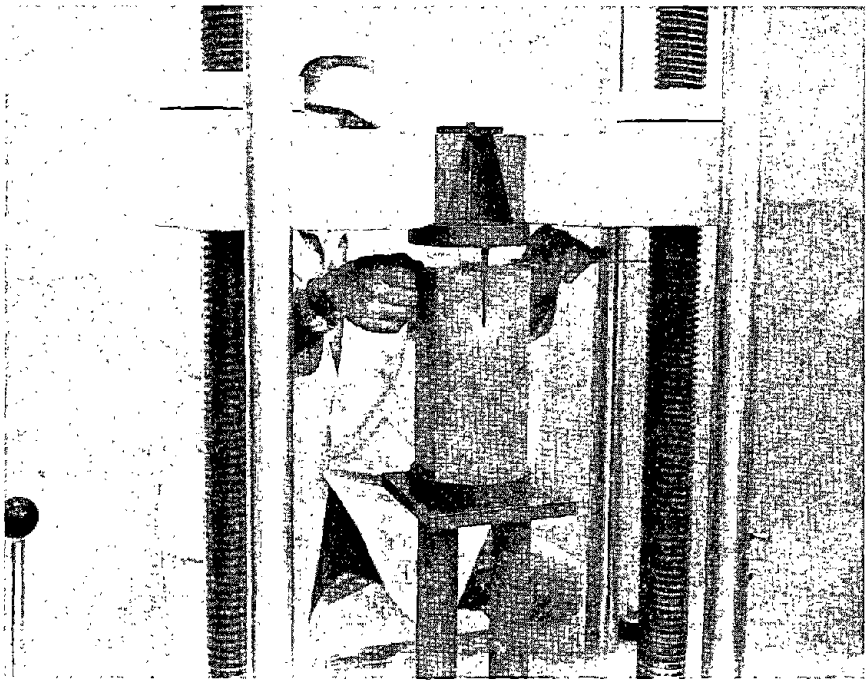

Figure 5.—Method of Loading Double Cantilever Beam Specimens and Measuring Displacement

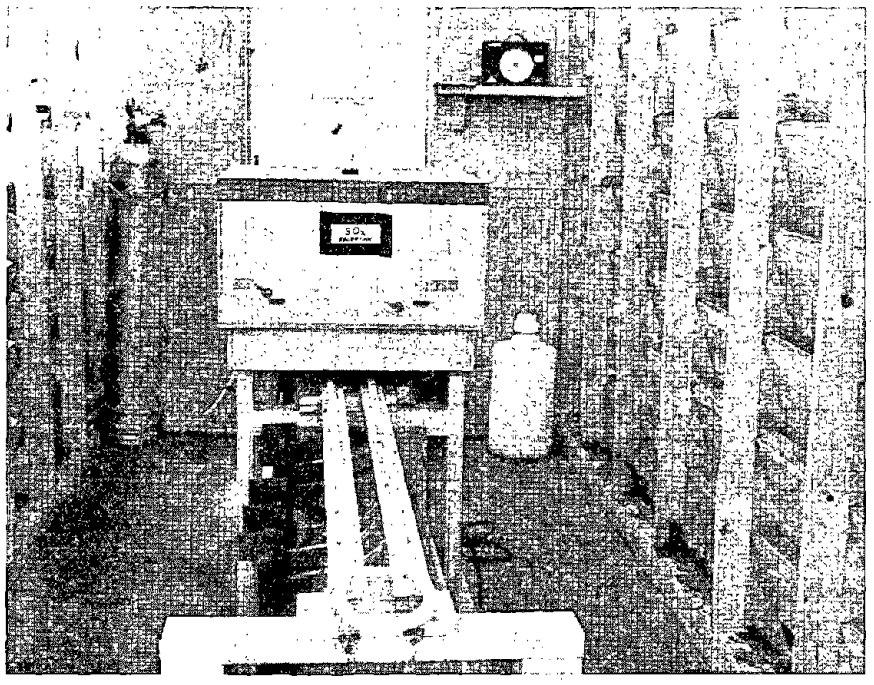

Figure 6.—Method of Distributing Aqueous Solution from Central Holding Tank to DCB Specimens

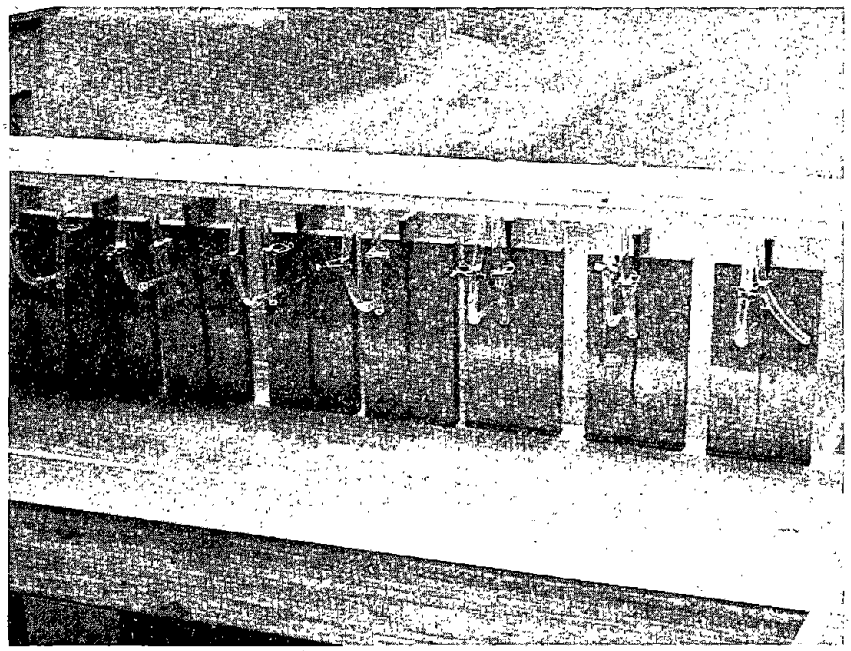

Figure 7.—Closeup Showing Method of Controlling Flow Rate with Hose Clamps and Glass Pipettes

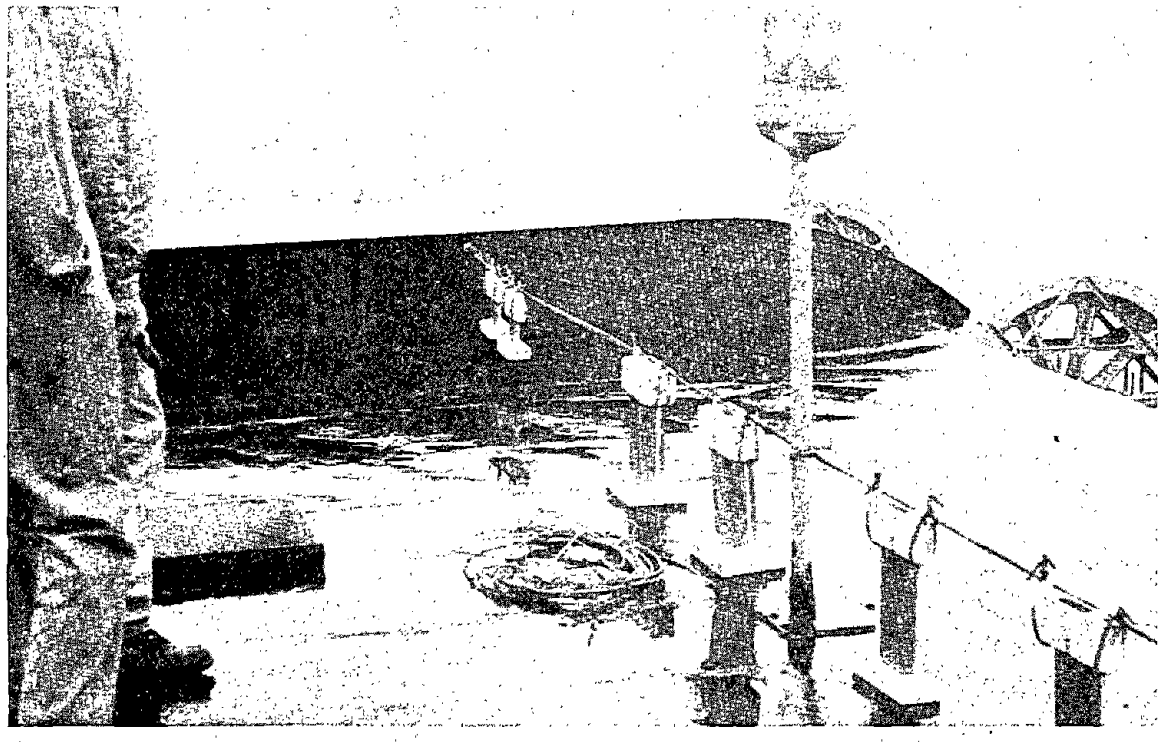

Specimens are Located on Top of North Tower
of West Drawspan

Figure 8.—Specimens Placed at Snohomish River Bridge

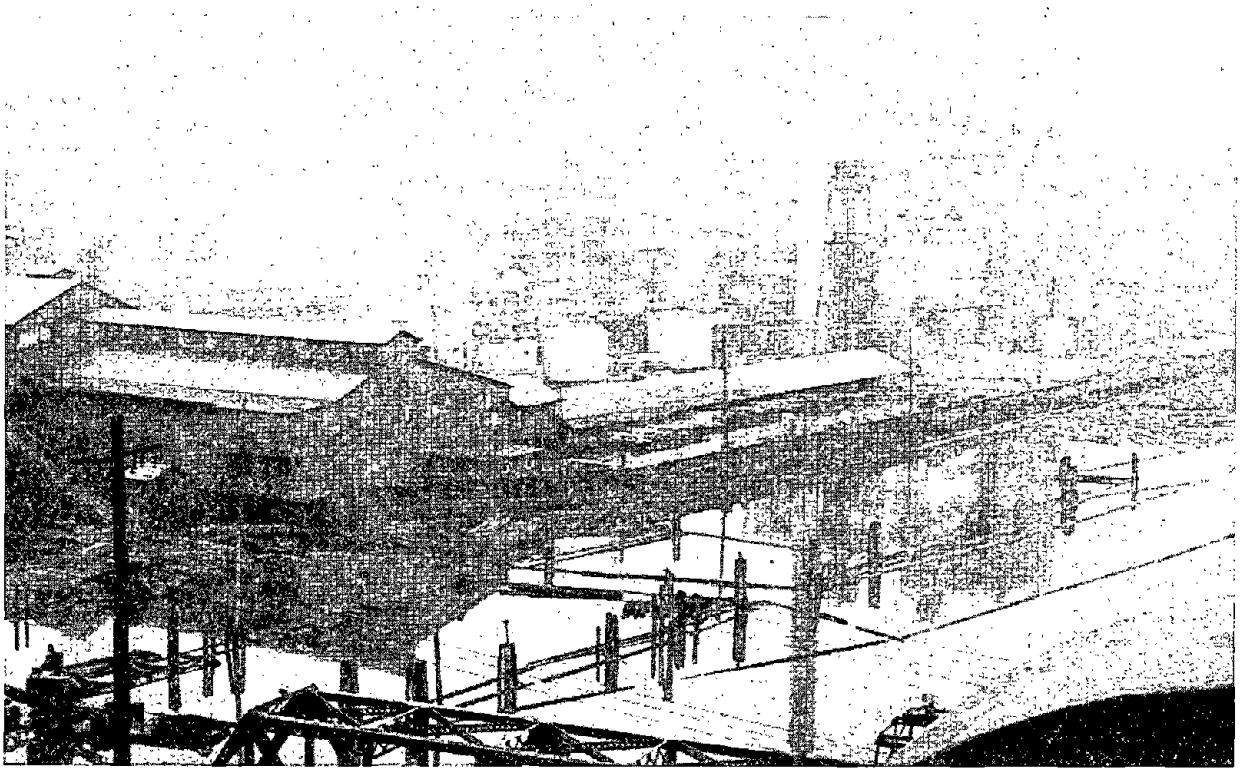

Figure 9.—Sulfide Pulp Mill as Seen from Specimen Location at Snohomish River Bridge (View Looking South)

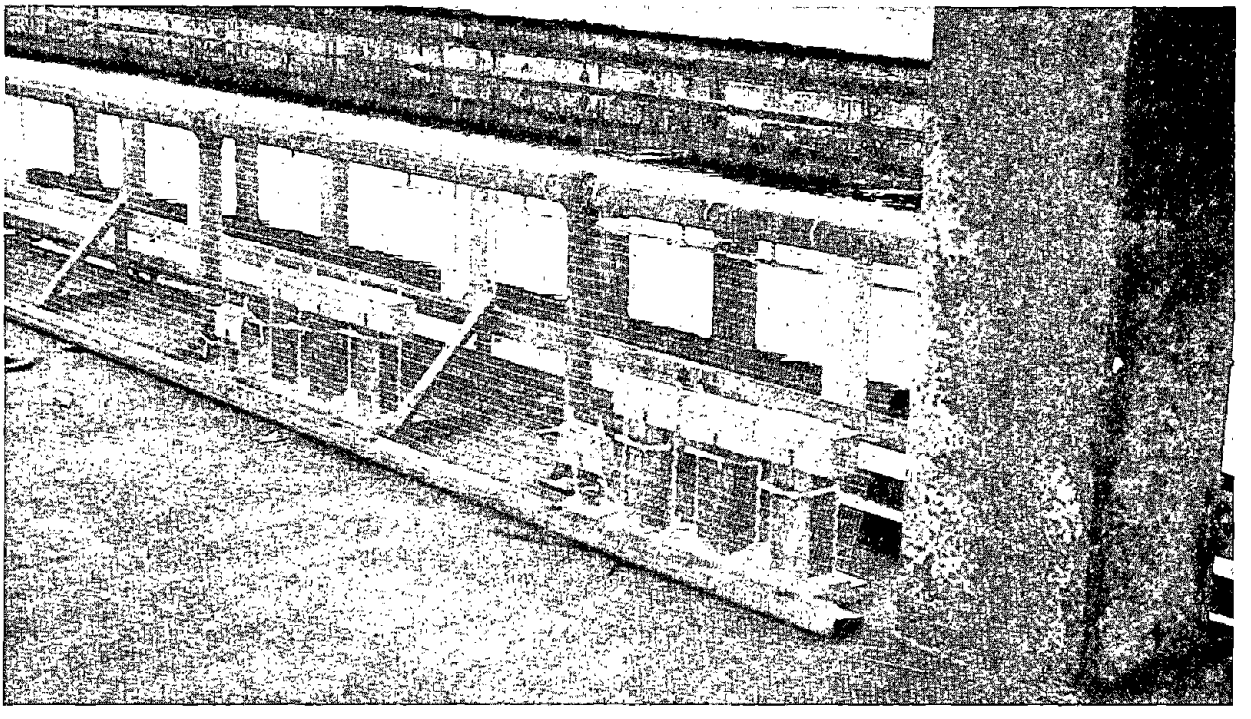

Wire Screen in Front of Specimens Prevents Waves from Washing Debris Into the Pool Between the South and North Floats.

Figure 10.—Specimens Placed on South Float of Hood Canal Floating Bridge

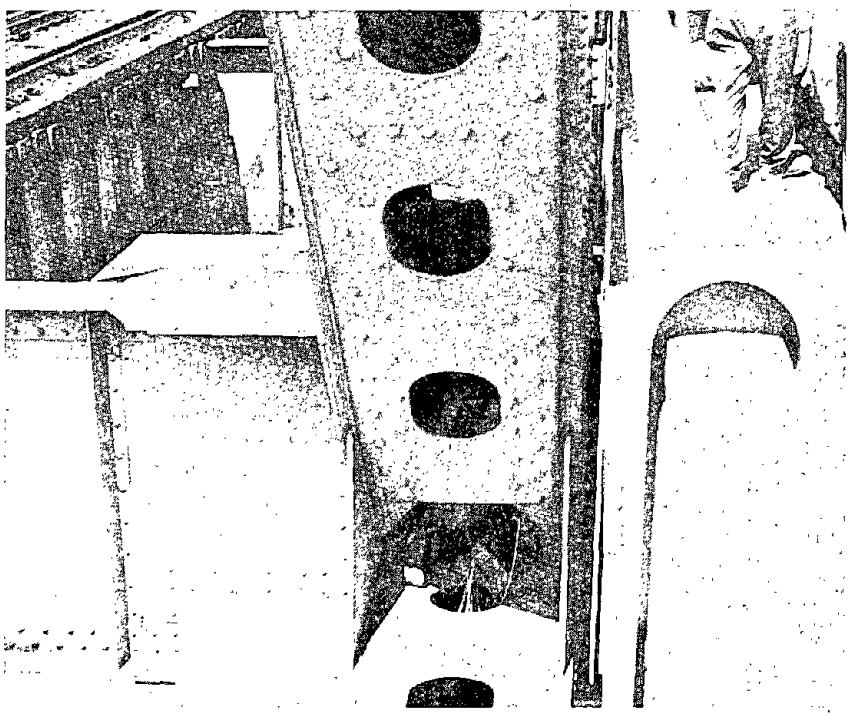

Specimens Were Placed 4 to 5 Ft Below the Roadway in the Space Formed by the Intersection of Vertical, Diagonal, and Horizontal Members.

Figure 11.—Specimen Location on North Side of Huey P. Long Memorial Bridge

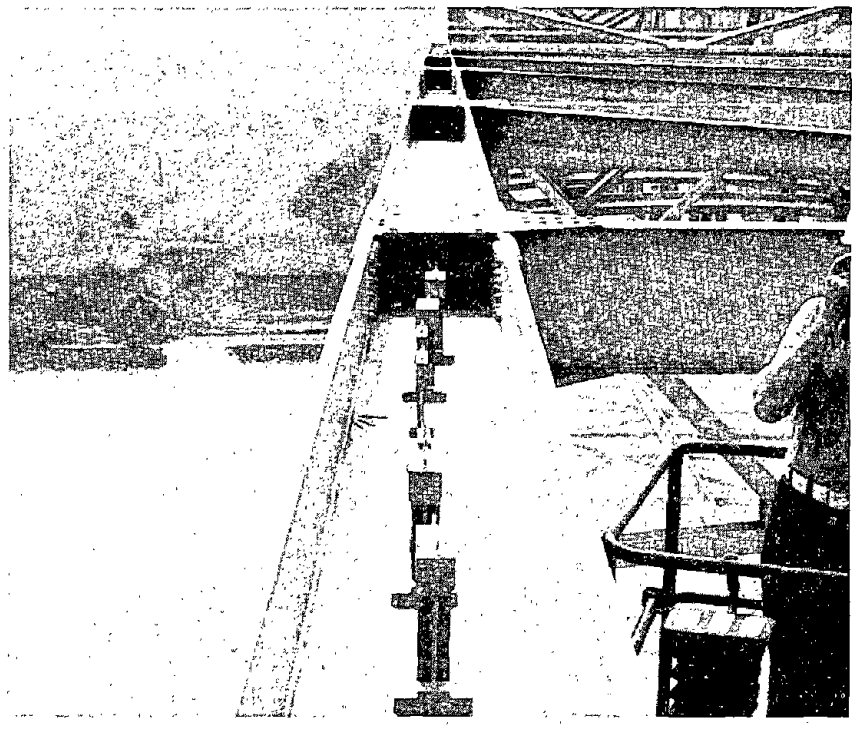

Specimens are Located on the Web of the Uppermost Beam at Midspan.

Figure 12.—Specimens Placed on Silver Memorial Bridge

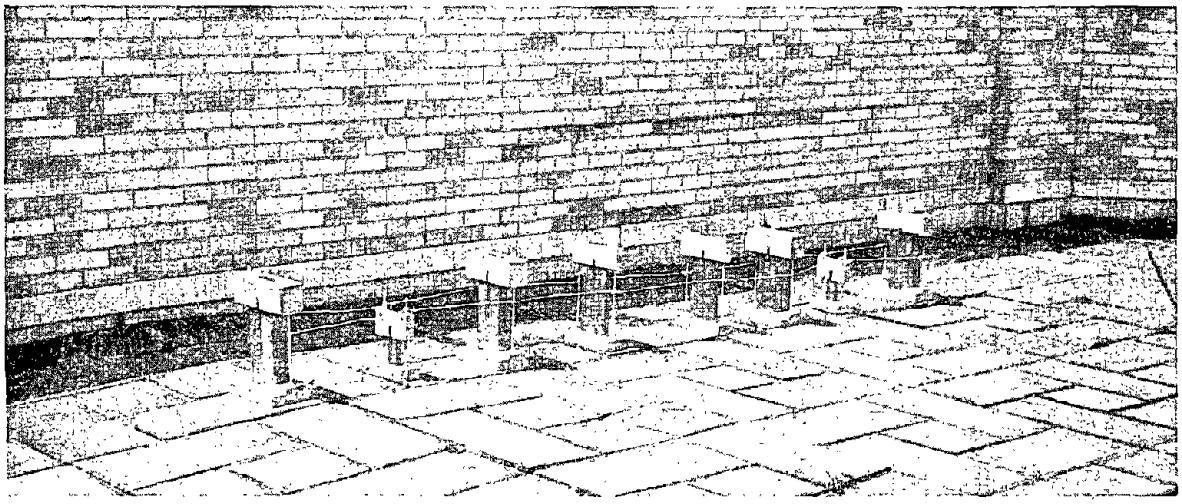

Specimens are Located on the Roof of the Northwest Wing.

Figure 13.—Specimens Placed at Franklin Institute Science Museum

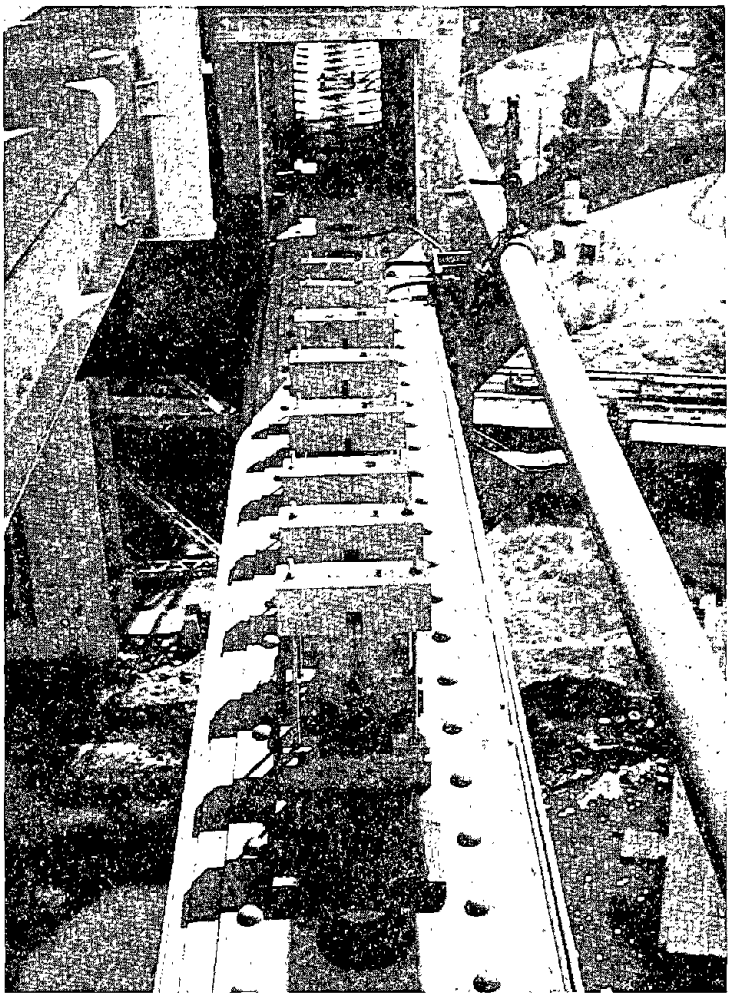

Specimens are Located on the West Side Near the South End of the Bridge 4 to 5 Feet Below Roadway

Figure 14.—Specimens Placed on West Carquinez Bridge

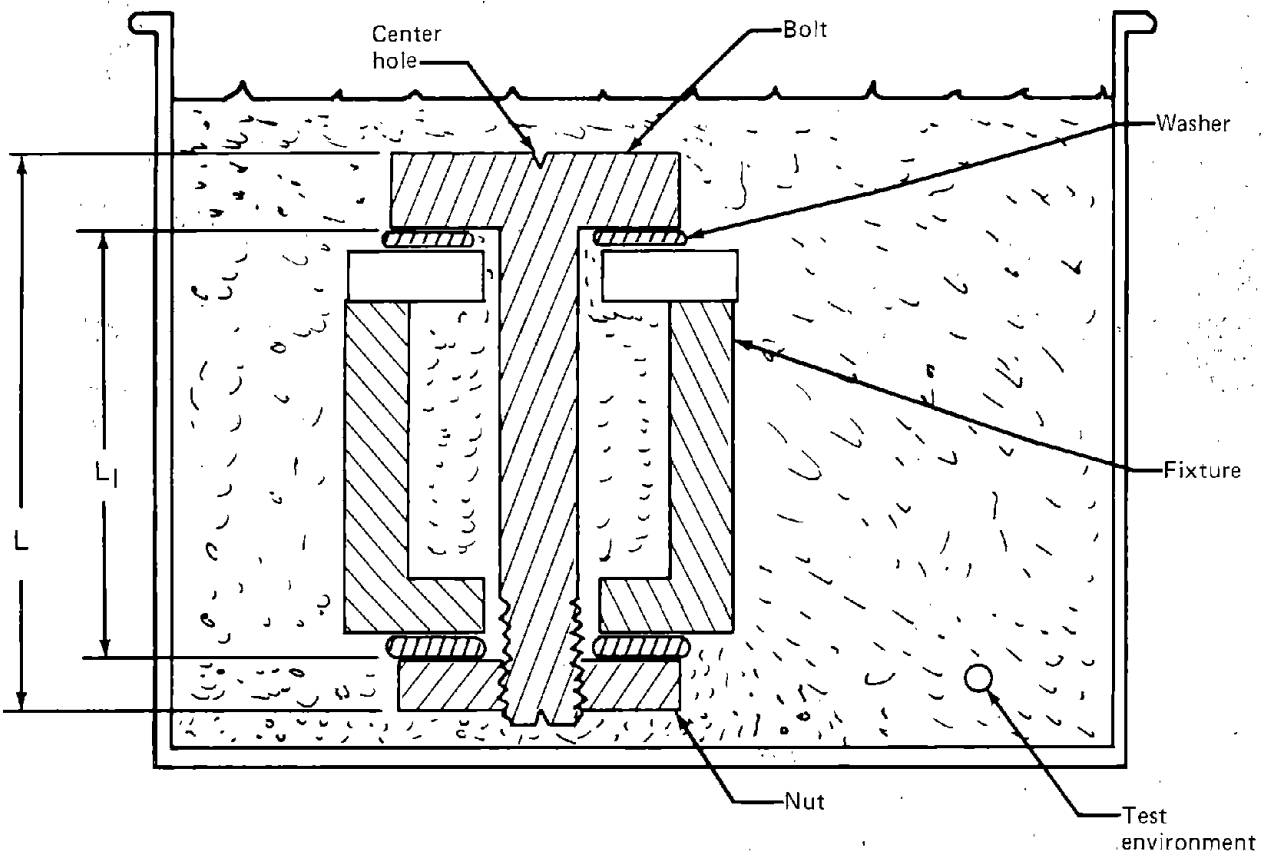

Figure 15.—Bolt Stress Corrosion Test Setup

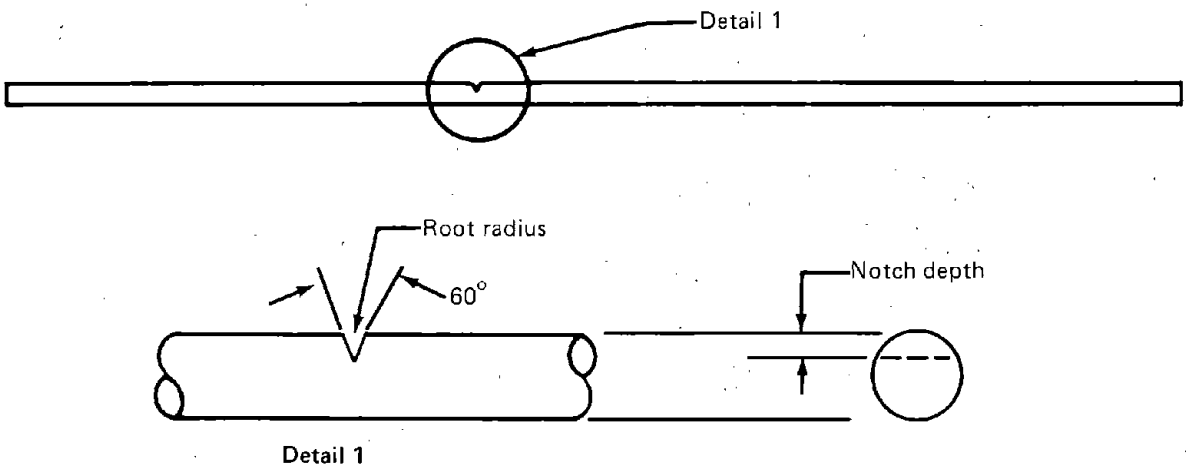

Figure 16.—Wire Specimen Notch Configuration

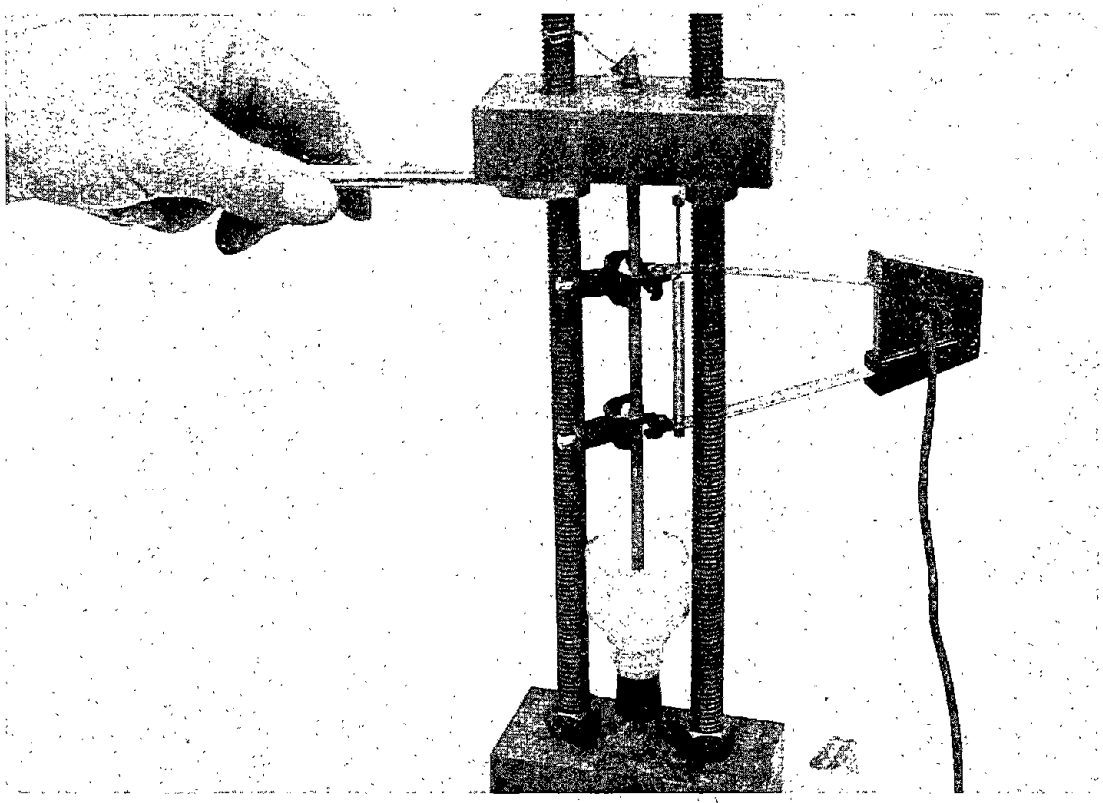

Figure 17.—3/16-In.-Diameter Wire Specimens Mounted in Test Fixtures with Attached Extensometer

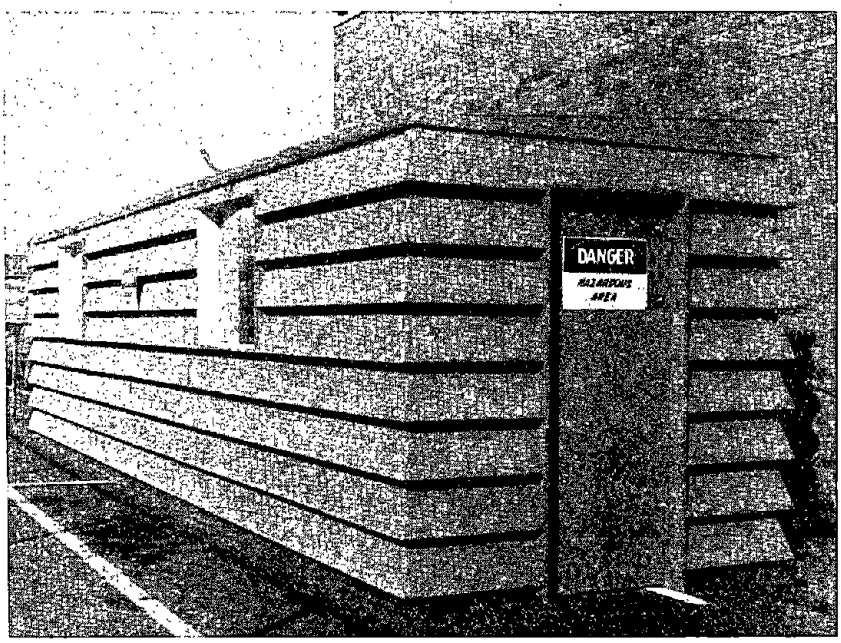

Figure 18.—Outdoor Facility for Sulfur Dioxide and Hydrogen Sulfide Testing Showing Overlapping Board Construction

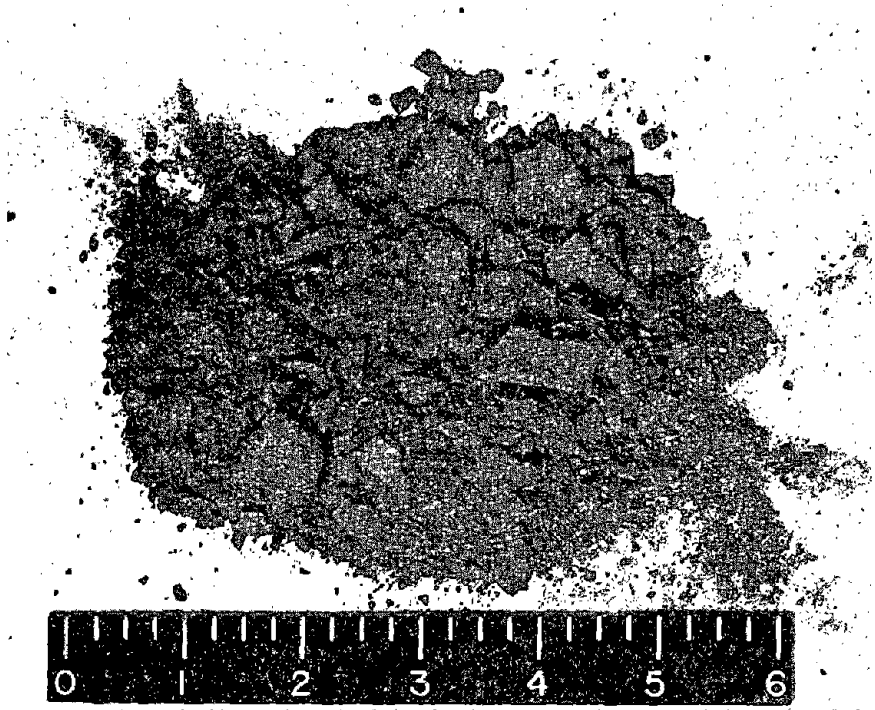

Material Shown Above and in Figure 20 was Taken in March 1975 from Between Pin Nut and Face of an Inside Hanger Bar (Field Location Designation L305).

Figure 19.—Corrosion Products Taken From West Carquinez Bridge, West Truss

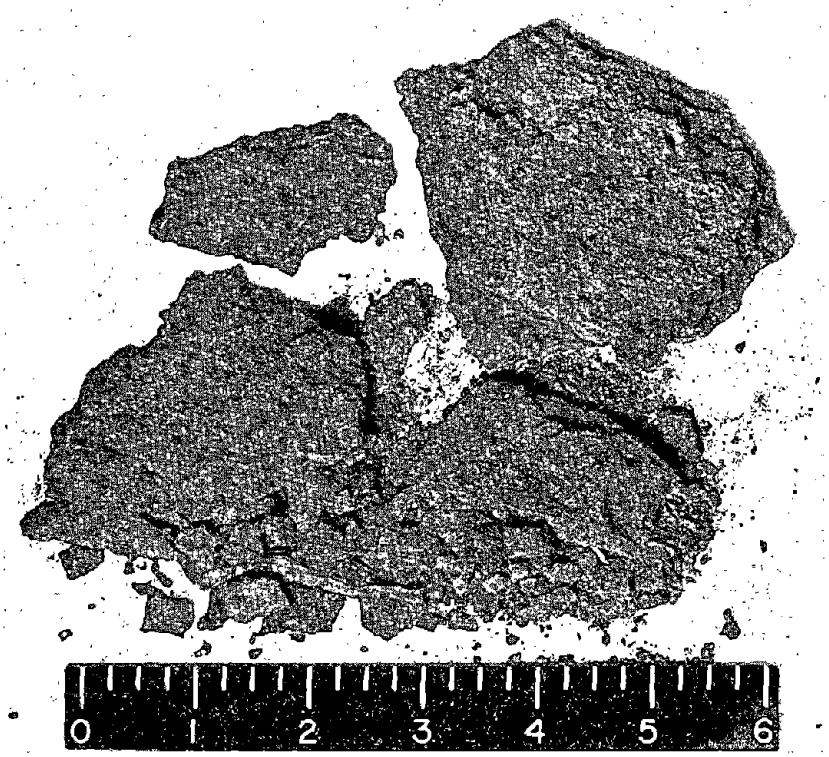

Figure 20.—Corrosion Products Taken From West Carquinez Bridge, East Truss

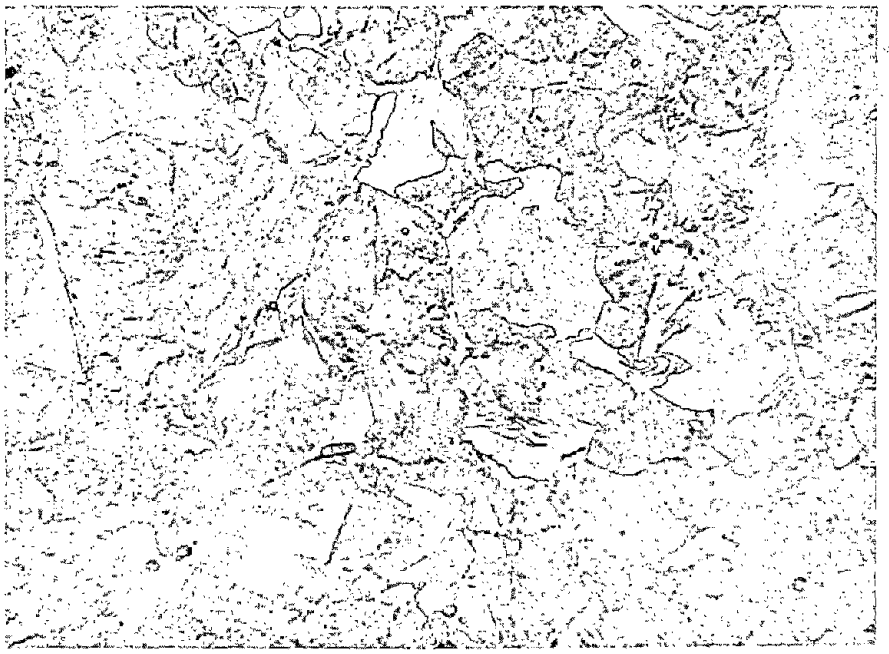

Etch 1% Nital Mag: 500X

Figure 21.—Typical Microstructure of 1035 Steel Taken From West Carquinez Bridge Eyebars (Specimen U16N0)

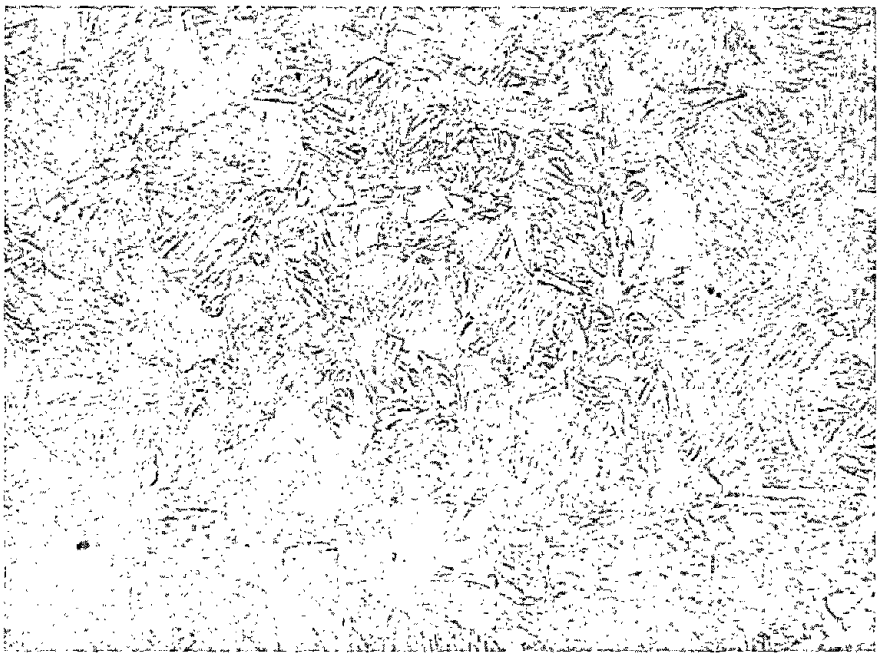

Etch 1% Nital Mag: 500X

Figure 22.—Typical Microstructure of Water Quenched A514 Type F Steel

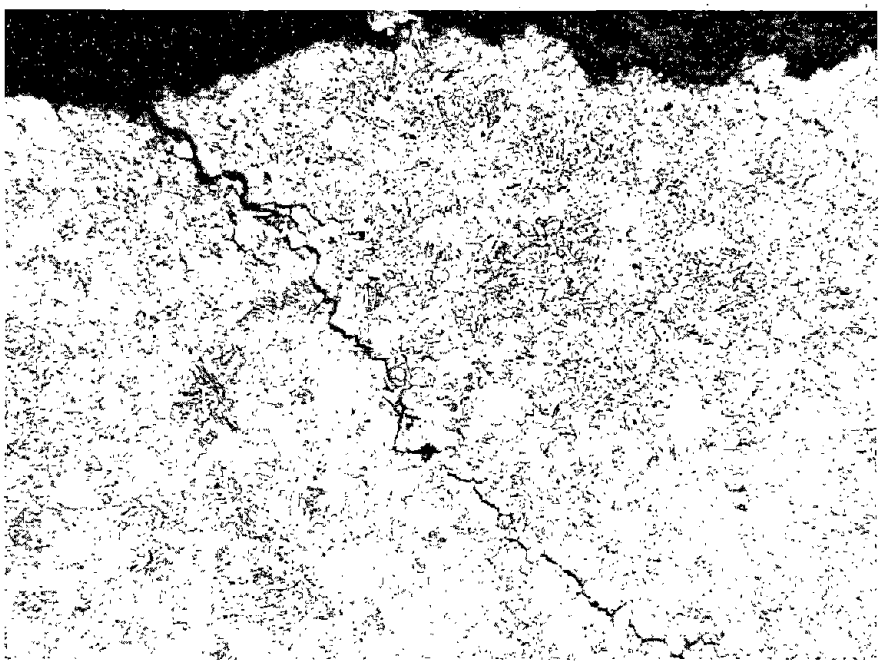

Etch 1% Nital Mag: 100X

(a) Intergrannular, Secondary Stress Corrosion Crack in Slow Cooled A514 Type F Steel

Figure 23.—Micrographs of Stress Corrosion Cracking in Steels Exposed to 5% Calcium Nitrate/0.25% Ammonium Nitrate Solution

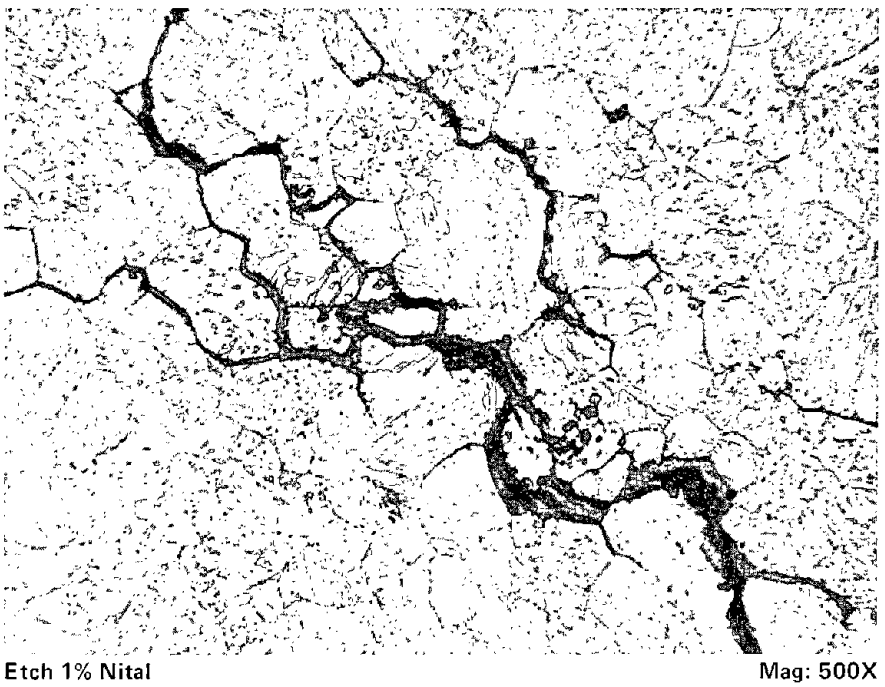

Etch 1% Nital Mag: 500X

(b) Intergrannular Cracking Along Grain Boundary Carbides in Slow Cooled A514 Type F Steel

Figure 23.—(Continued)

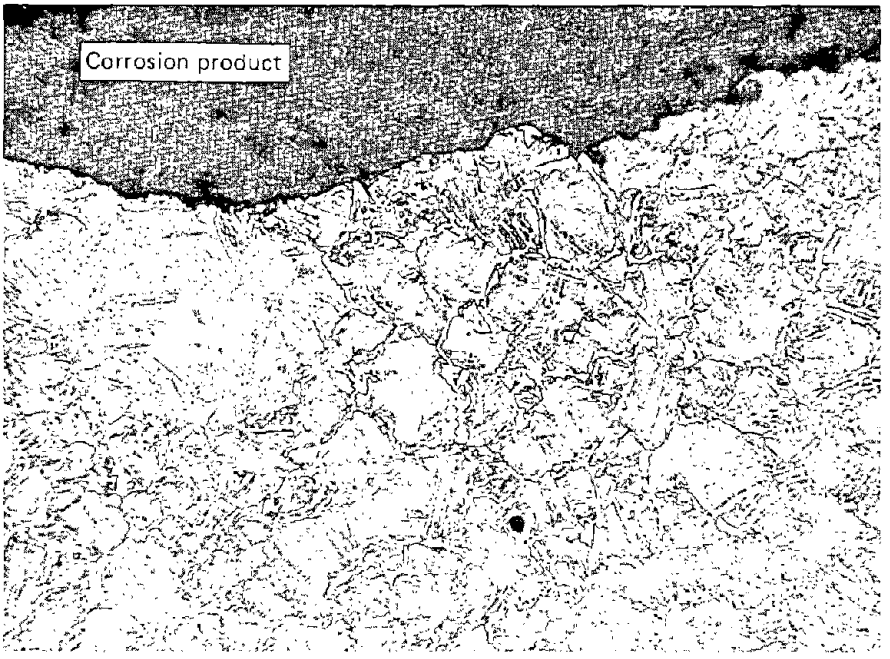

Etch 1% Nital Mag: 500X

(c) Pro-eutectoid Grain Boundary Ferrite in Water-Quenched A441 Steel (Massive Corrosion Product Obscures Crack Morphology)

Figure 23.—(Continued)

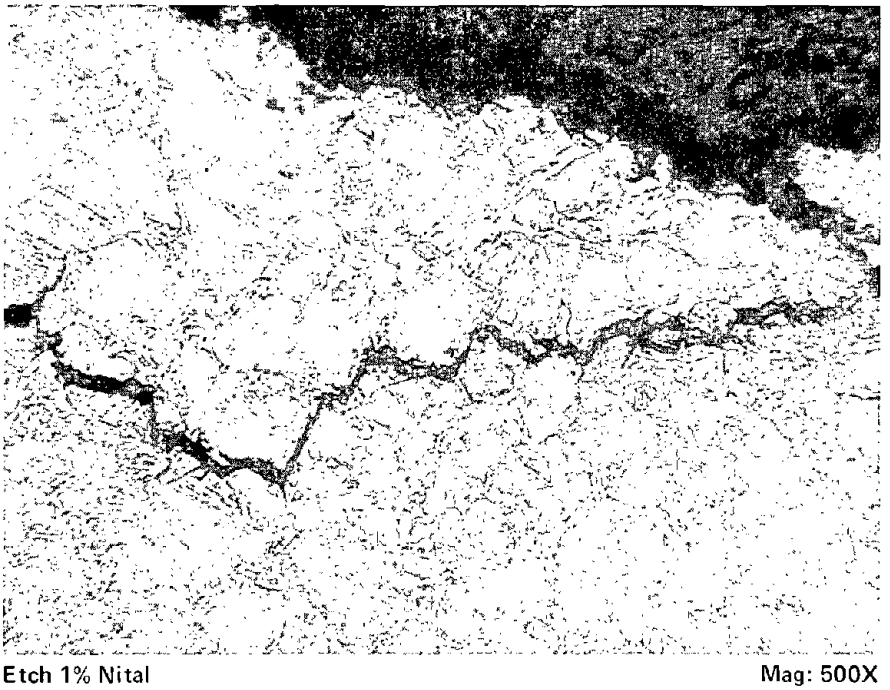

Etch 1% Nital Mag: 500X

(d) Intergrannular Secondary Stress Corrosion Crack in Water Quenched A441 Steel

Figure 23.—(Concluded)

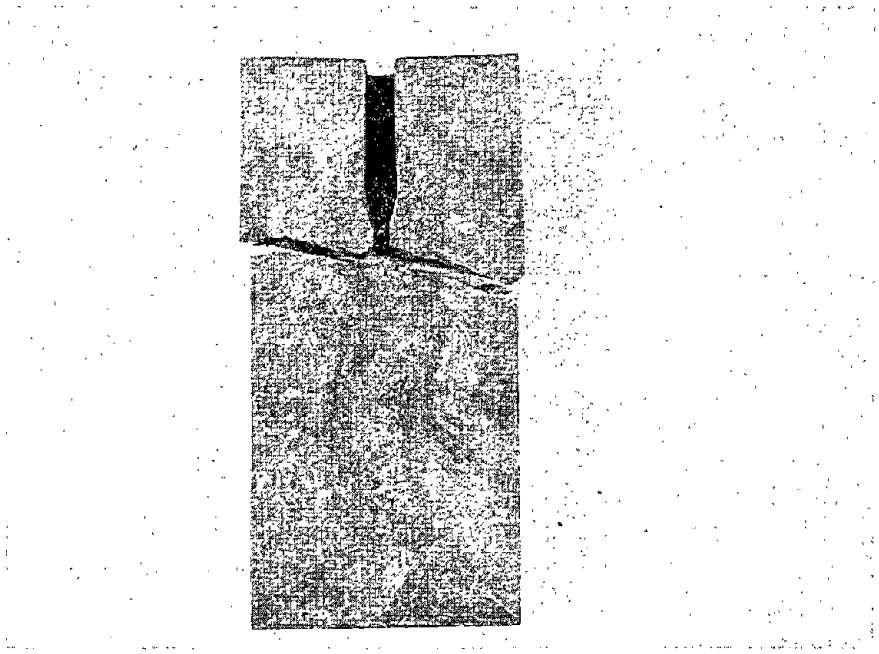

Mag: 2.3X

(a) View Showing Fracture Branching at Crack Tip

Figure 24.—Crack Branching in Water Quenched A514 Type F Steel Exposed to 5% Calcium Nitrate/0.25% Ammonium Nitrate Solution

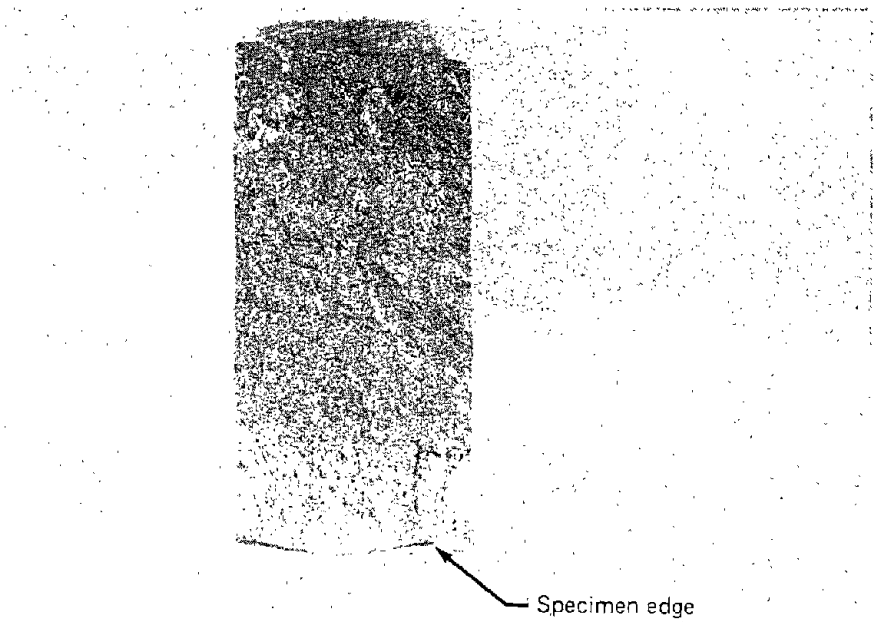

Mag: 2.4X

(b) Right Fracture Face of Specimen Shown in (a)

Figure 24—(Concluded)

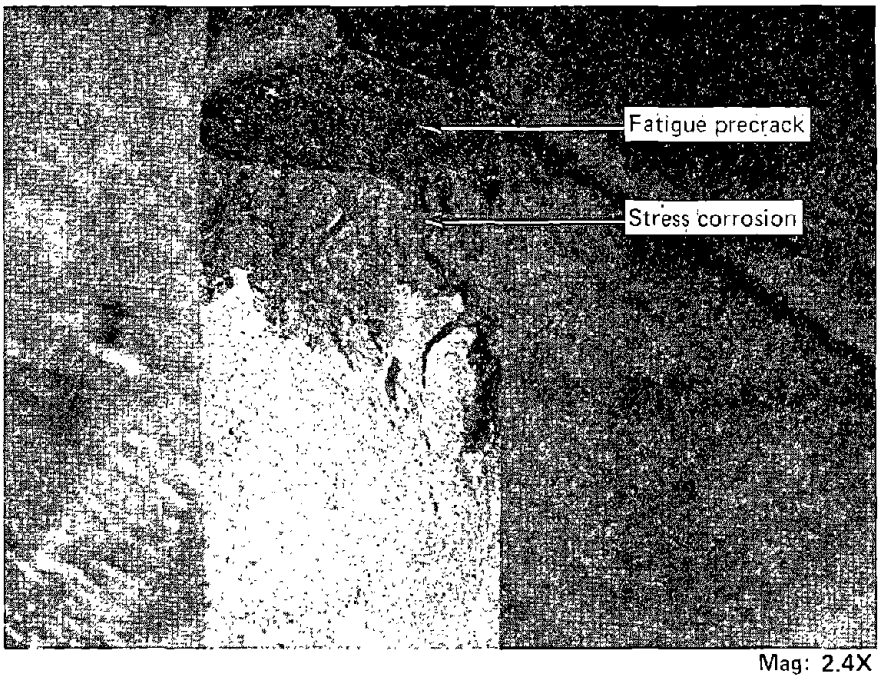

Mag: 2.4X

(a) Slow Cooled A514 Type F Steel

Figure 25.—Stress Corrosion Cracking in Steels Exposed to 5% Calcium Nitrate/0.25% Ammonium Nitrate Solution

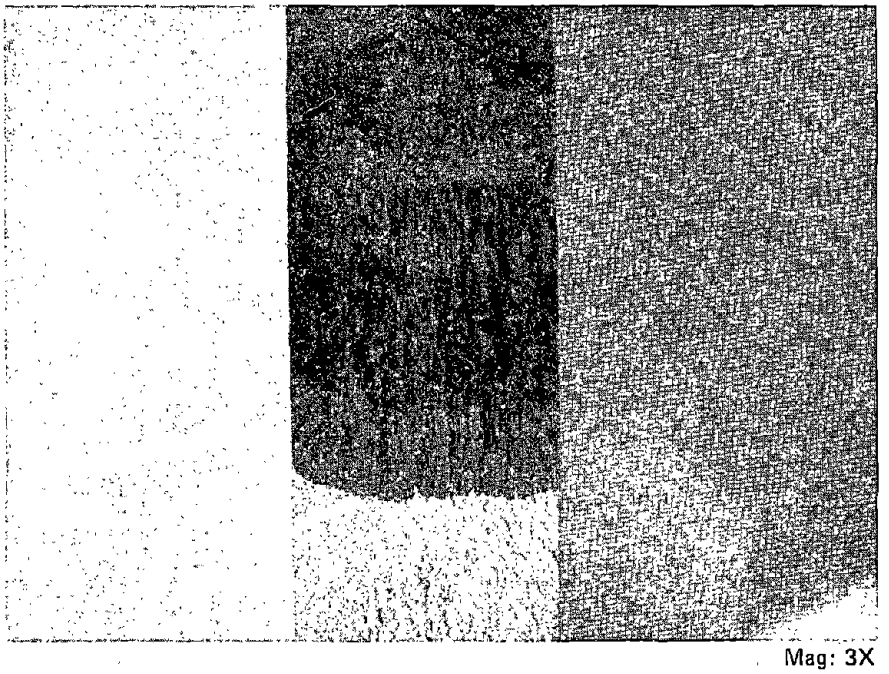

Mag: 3X

(b) Slow Cooled A441 Steel

Figure 25.—(Concluded)

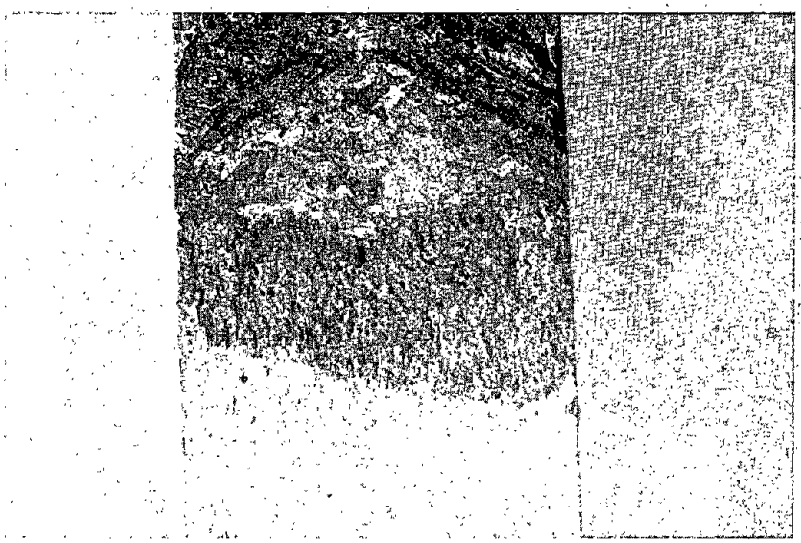

Figure 26.—Stress Corrosion Cracking in A517 Grade H Steel Exposed to 3.5% Sodium Chloride/0.5% Acetic Acid/Saturated H_2S Solution

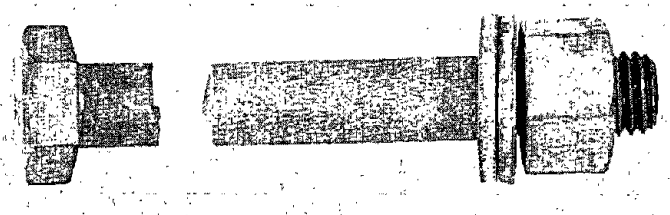

(a) Shank Failure of Bare ASTM 490, 3/4-10 UNC Bolt After 72 Hour Submersion (Specimen G64)

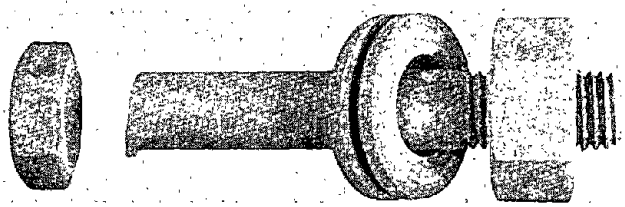

(b) Head-to-Shank Failure of Mechanically Galvanized ASTM 490, 3/4-10 UNC Bolt After 480 Hour Submersion (Specimen M63)

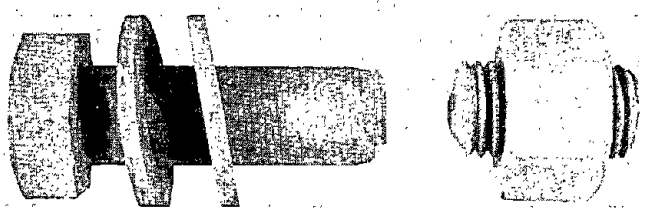

(c) Thread Root Failure of Bare ASTM 325, 7/8-9 UNC Bolt After 672 Hour Submersion (Specimen B74)

Figure 27.—Failed Bolts Exposed to 3.5% Sodium Chloride/0.5% Acetic Acid Saturated with H_2S

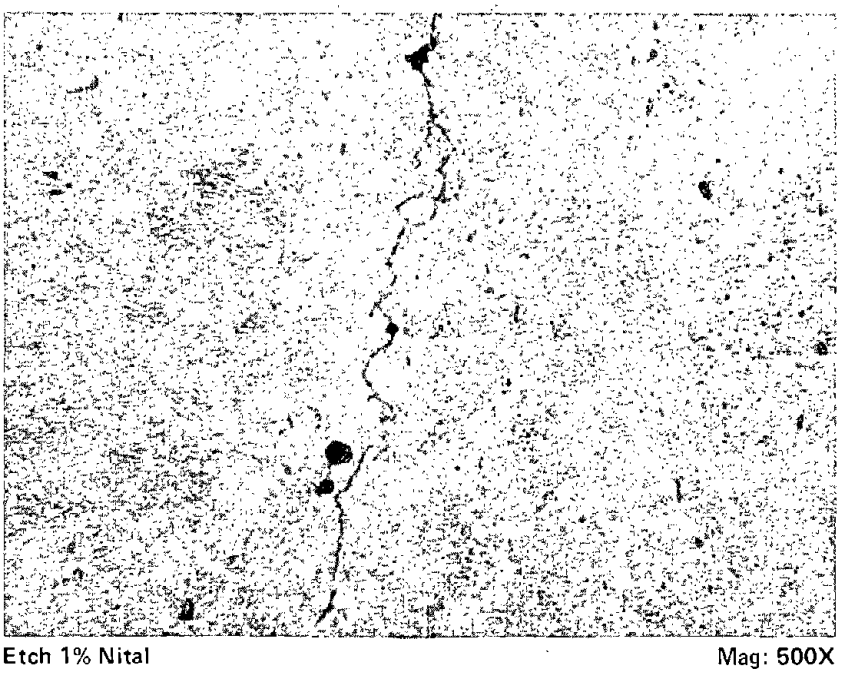

Figure 28.—Micrograph from Section of ASTM 490 Bolt Showing Intergrannular Secondary Cracking (Specimen B64)

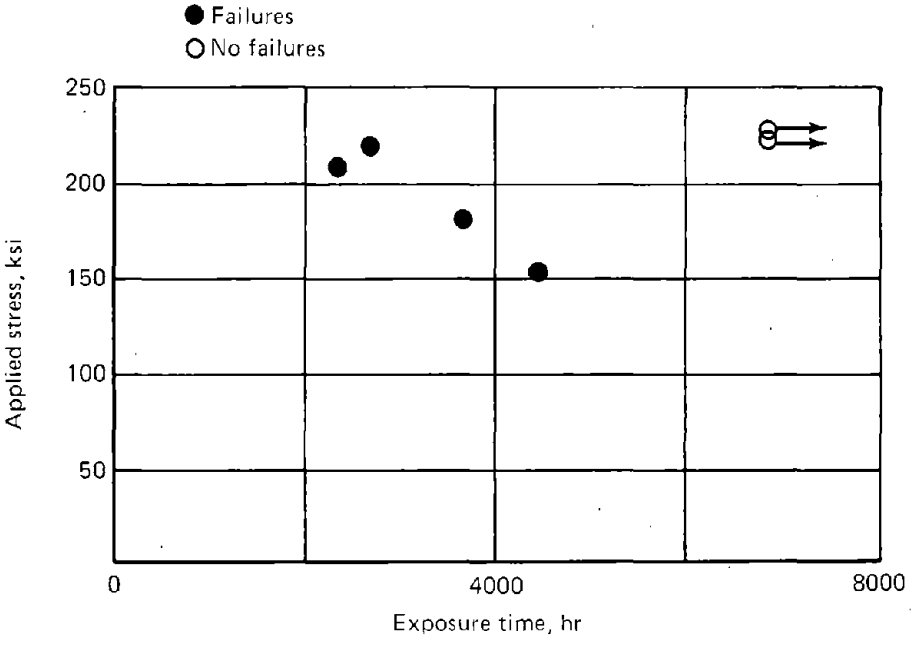

Figure 29.—Time to Failure for Bare Prestressing Wire Exposed to 5% Calcium Nitrate/ 0.25% Ammonium Nitrate Solution

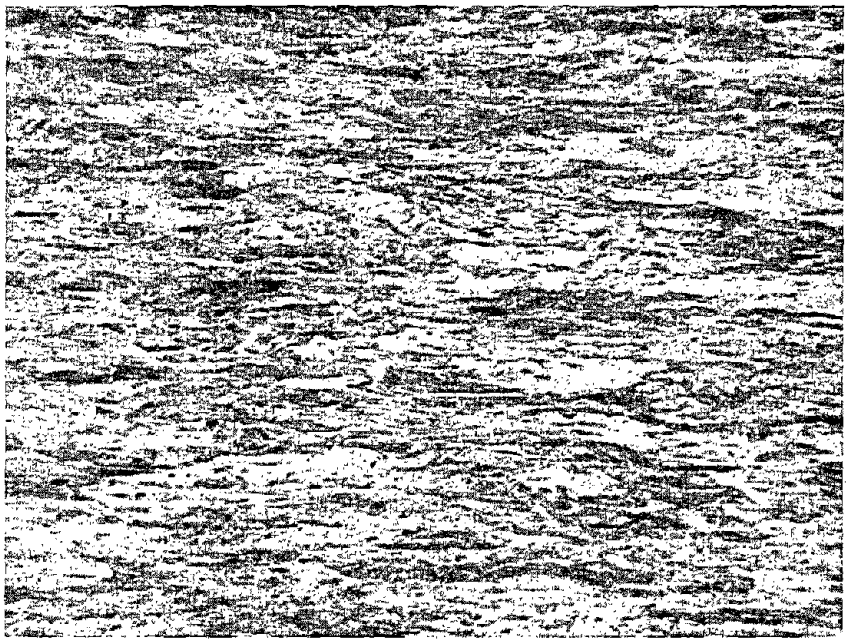

Etch 1% Nital Mag: 500X

Figure 30.—Typical Cold Worked Microstructure of Prestressing Wire

Table 1.—Steels Recommended for Testing from Phase I (ref. 2)

Steel	Reasons for selection
A36	This steel is resistant to stress corrosion cracking in the highway environment but tests are required to provide a reference baseline.
A8	Tensile strength range (90-115 ksi) is close to that definitely known to be susceptible to cracking in H_2S. High carbon (0.43% max) and nickel (3%-4%) contents may increase susceptibility to H_2S cracking, and high carbon is detrimental to SCC resistance in chloride solutions
A242	One high-phosphorus-content steel is selected, because phosphorus has an adverse effect on stress corrosion resistance. Other weathering steels to A588 will also be tested.
A441	Widely used High-strength, low-alloy steel for which SCC resistance has not been established.
A514	Steels of this type are known to be susceptible to cracking in saturated H_2S solution, but threshold stress intensity values are not established. There is a scarcity of data for other environments. Four types are selected: Type E—high chromium content but nickel absent Type F—high alloy content with nickel (0.8%-1.0%) present Type H—intermediate alloy content Type J—low allow content Nickel-free and nickel-containing types have been selected since nickel is reported to have an adverse effect on H_2S cracking resistance. Type J has a relatively high molybdenum content; this element is reported to have an adverse effect on SCC in chloride environments. Chromium is also reported to have an adverse effect in this environment. Composition and strength characteristics are similar to A517, and will allow for an assessment of these steels.
A572	These are recently introduced high-strength, low-alloy steels for which only a small amount of SCC data is available. Three types are selected with a minimum yield strength of 60 ksi: Type 1—strengthened by columbium Type 2—strengthened by Vanadium Type 4—strengthened by vanadium and nitrogen Also, one steel to grade 50 is included.
A588	No data are available for these recently introduced high-strength, low-alloy steels. Three grades are selected: Grade A—chromium bearing with nickel absent Grade E—nickel bearing with chromium absent Grade H—contains significant amount of practically all alloying elements used in specification A588 These alloys are selected for the same reasons as were discussed for A514. Grade E also has a high Cu content, which is reported to adversely affect cracking resistance in nitrates.
AISI 1035	This steel, heat treated to a minimum yield strength of 50 ksi, has been used for eyebars. In view of the critical nature of some applications, and the prior stress corrosion failure of a higher strength eyebar, testing is considered necessary.

Table 2.—Chemical Composition and Thickness of Structural Steels Tested in Phases IIA and IIB

Steel	Supplier and heat number	Plate thickness, in.	Chemical composition (supplier's analysis)						
				C	Mn	Si	S	P	Other
A36	Kaiser[a] 28532	3	Plate	0.18	0.97	0.22	0.027	0.008	—
			Specification	0.27-max	0.85-1.20	0.15-0.30	0.05-max	0.04-max	—
A441	U.S. Steel[d] 97B993	3	Plate	0.17	1.16	0.24	0.023	0.025	0.36 Cu, 0.08V
			Specification	0.22-max	0.85-1.25	0.30-max	0.05-max	0.04-max	0.20 min Cu, 0.20 min V
A514 type E	Armco[a] 50478	3	Plate	0.20	0.64	0.30	0.015	0.010	1.91 Cr
			Specification	0.12-0.20	0.40-0.70	0.20-0.35	0.04-max	0.035-max	1.40-2.0 Cr, 0.40-0.60 Mo, 0.04-0.10 Ti, 0.20-0.40 Cu, 0.0015-0.005B
A514 type F	U.S. Steel[a] 71D653	3	Plate	0.17	0.85	0.26	0.020	0.010	0.83 Ni, 0.53 Cr
			Specification	0.10-0.20	0.60-1.00	0.15-0.35	0.04-max	0.035-max	0.70-1.00 Ni, 0.40-0.65 Cr, 0.40-0.60 Mo, 0.03-0.08 V, 0.15-0.50 Cu, 0.002-0.006B
A517 Grade H	Lukens[b]	2¼	Plate	0.21	1.09	0.29	0.019	0.010	0.37 Ni, 0.53 Cr, 0.30 Mo, 0.05V, 0.004 B
			Specification	0.12-0.21	0.95-1.30	0.20-0.35	0.04-max	0.035-max	0.30-0.70 Ni, 0.40-0.65 Cr, 0.20-0.30 Mo, 0.03-0.08 V, 0.0005-0.005 B
A514 type J	Bethlehem[a] 516A0689	1	Plate	0.18	0.58	0.27	0.024	0.012	0.60 Mo, 0.0028B
			Specification	0.12-0.21	0.45-0.70	1.20-0.35	0.04-max	0.035-max	0.50-0.65 Mo, 0.001-0.005 B

Table 2.—(Concluded)

Steel	Supplier and heat number	Plate thickness, in.	Chemical composition (supplier's analysis)						
				C	Mn	Si	S	P	Other
A572 grade 50, type 2	U.S. Steel[d] 93B342	1	Plate	0.22	1.09	0.23	0.023	0.015	0.8 V
			Specification	0.23-max	1.35-max	0.30-max	0.05-max	0.04-max	0.01-0.10 V
A572 grade 60, type 4	Armco[c] 85768	1	Plate	0.20	1.42	0.02	0.012	0.010	0.084 V, 0.010 N
			Specification	0.26-max	1.35-max	0.30-max	0.05-max	0.04-max	0.01-0.10 V, 0.015 N, Min ratio V/N = 4:1
A588 grade A	U.S. Steel[d] 96B484	3	Plate	0.16	1.20	0.30	0.015	0.011	0.60 Cr, 0.22 Cu, 0.07 V
			Specification	0.10-0.19	0.90-1.25	0.15-0.30	0.05-max	0.04-max	0.40-0.65 Cr, 0.25-0.40 Cu, 0.02-0.10 V
AISI 1040	U.S. Steel[a] 98B322	1¼	Plate	0.44	0.80	0.17	0.012	0.009	—
			Specification	0.36-0.45	0.60-0.90	—	0.05-max	0.04-max	—
1035	Carquinez bridge eyebars	1½	U16NO[e]	0.36	0.72	0.12	0.062	0.01	0.03 Cu
			U14NO[e]	0.30	0.70	0.12	0.053	0.01	0.07 Cu
			U14SO[e]	0.28	0.66	0.13	0.033	0.01	0.03 Cu

[a]Obtained from steel stockist

[b]Obtained from California State Highway Dept.

[c]Obtained from a steel user

[d]Obtained from U.S. Steel Supply Division

[e]Eyebar specimen number

Table 3.—Tensile Properties of Structural Steel (ref. 3)

Steel	Test conducted by	TYS, ksi	TUS, ksi	Elongation, %	Reduction of area, %
A36	Supplier	37.12 37.85	66.59 67.98	31 25	– –
	Boeing	31.0 29.6	68.1 66.3	18 18	56 56
	Specification	36.0 min	58.0-80.0	[a]23 min	–
A441	Supplier	58.1	80.3	33	–
	Boeing	53.0 51.0	79.1 78.1	30 30	57 59
	Specification	42.0 min	63.0 min	[a]21 min	–
A514 type E	Supplier	110.3	122.3	19.5	–
	Boeing	114.7 106.6	126.8 121.5	34 35	61 60
	Specification	90.0 min	105.0-135.0	[a]17 min	–
A514 type F	Supplier	110.8	123.3	19.0	–
	Boeing	110.0 107.4	120.1 118.5	22 22	63 66
	Specification	90.0 min	105.0-135.0	[a]17 min	–
A517 grade H	Boeing	122.9 120.1	134.7 132.2	16 16	46 47
	Specification	100.0-min	115.0-135.0	16 –	– –
A514 type J	Supplier	113.7	117.8	20	–
	Boeing	108.5 107.3	124.0 123.2	20 22	60 59
	Specification	100.0 min	115.0-135.0	[a]18 min	– –
A572 grade 50	Supplier	60.6	88.0	31	–
	Boeing	47.3 47.4	76.0 76.4	33 34	68 69
	Specification	50.0 min	65.0 min	[a]21 min	–
A572 grade 60	Supplier	65.4	85.1	27	–
	Boeing	66.4 61.7	83.0 82.8	30 30	61 61
	Specification	60.0 min	75.0 min	[a]18 min	–
A588 grade A	Supplier	51.8	77.5	33	–
	Boeing	49.1 50.6	77.5 76.9	28 32	63 63
	Specification	50.0 min	70.0 min	[a]21 min	–
AISI 1040	Boeing[b]	64.6 65.0	102.8 102.5	26 27	47 48

[a]2-in. gage length

[b]Austentized 1550° F for 1.5 hrs, water quenched, and tempered at 1225° F

Table 4.—Chemical Composition of Typical Bolts

Material	Chemical composition				
	C	Mn	S	P	Si
A490 bare, 3/4 10 UNC	0.41	–	0.026	0.020	–
A490 specification	0.28-0.50	–	0.045 max	0.045 max	–
A325 bare, 7/8 9 UNC	0.35	0.52	0.024	0.01	–
A325 dip galvanized, 7/8 9 UNC	0.35	0.76	0.025	0.010	0.23
A325 bare, 1-1/8 7 UNC	0.32	1.22	0.026	0.013	0.20
A325 dip galvanized, 1-1/8 7 UNC	0.30	1.19	0.022	0.012	0.20
A325 specification, type 1	0.27 min	0.47 min	0.058 max	0.048 max	–

Table 5.—Tensile Properties of A325 and A490 Bolts

Bolt	Description	TYS, ksi	TUS, ksi	Elongation, %	Reduction of area, %
A490	3/4 10 UNC bare	157.3 148.5 150.8	167.3 158.6 160.2	16 18 18	60 60 56
	1/2 to 1-1/2 in. specification	130 min	150-170	14 min	40 min
A325	7/8 9 UNC bare	87.0 103.4 97.8	111.9 118.4 112.9	25 17 18	70 63 65
	7/8 9 UNC dip galvanized	119.5 96.3	136.2 122.7	17 20	56 54
	1/2 to 1 in. specification	92 min	120 min	–	–
A325	1-1/8 7 UNC bare	88.3 90.1	110.8 111.3	19 20	58 57
	1-1/8 7 UNC dip galvanized	78.9 87.0	114.8 108.3	18 20	56 60
	1/2 to 1 in. specification	81 min	105 min	14 min	35 min

Table 6.—Chemical Composition of Wire Materials

Cable wire	Chemical composition						
	C	S	P	Mn	Si	Ni	Cr
Bare suspension wire, 0.188 in. diameter	0.74	0.033	0.01	0.78	–	0.11	0.10
Dip galvanized suspension wire, 0.192 in. diameter	0.65	0.026	0.01	0.69	–	0.10	0.10
Electrogalvanized suspension wire, 0.187 in. diameter	0.69	0.024	0.01	0.70	–	0.10	0.10
Galvanized prototype suspension wire, 0.108 in. diameter	0.78	0.030	–	0.20	0.10	0.01	0.10
Bare prestressing wire, 0.128 in. diameter	0.76	0.021	0.01	0.72	–	0.11	0.10

Table 7.—Wire Tensile Properties Before and After Straightening

Material	Straightening	TUS, ksi	TYS, ksi	Elongation in 2 in., %
Bare suspension cable wire, 0.188 in. diameter	None	247.6 246.7	193.8 194.3	6 7
	[a]0.9–1.1	[b]236.3 [b]223.3	234.1 223.3	(b) (b)
Dip galvanized suspension cable wire, 0.192 in. diameter	None	216.6 217.6	161.3 139.9	10 10
	[a]0.7–1.1	[b]202.4 [b]197.7	191.7 188.7	(b) (b)
Electrogalvanized suspension cable wire 0.187 in. diameter	None	227.4 228.4	176.6 183.1	9 10
	[a]1.1–1.2	[b]202.6 [b]223.2	184.6 186.3	(b) (b)
Galvanized prototype suspension cable wire, 0.108 in. diameter	None	197.8 197.3	159.3 138.5	8 6
	[a]0.5	222.2 215.8 222.8 212.5	199.0 192.6 198.6 188.5	7 5 8 5
Bare prestressing cable wire 0.128 in. diameter	None	265.5 [b]272.3	246.1 246.9	8 (b)

[a]Percent of permanent set after stretch straightening

[b]Grip failure

Table 8.—Specimen Identification

Specimen I.D. XX XX
- XX: Steel code
- XX: Specimen number

Steel	Steel code	Specimen numbers	Phase	Nominal specimen dimension, in.[a] b	2h	W	Conditions
A36	AD	1 through 11	IIA	2.90	4.93	10.25	As received
	AA	1 through 12	IIB	2.90	4.90	10.40	As received
A441	CD	1 through 11	IIA	2.90	4.93	10.25	As received
	CCW	3A through 6A 3B through 6B	IIA	1.00	2.00	7.06	Cold worked
	CC	1 through 8	IIB	0.50	2.00	5.00	Water quenched from 1700°F to simulate weld
A514 type E	BD	1 through 11	IIA	2.90	4.93	10.25	As received
	BB	1 through 18	IIB	0.75	2.00	5.00	As received
A514 type F	FD	1 through 11	IIA	2.90	4.93	10.25	As received
	FCW	3A through 6A 3B through 6B	IIA	1.00	2.00	7.06	Cold worked
	FF	1 through 8	IIB	0.50	2.00	4.25	Water quenched from 1700° F to simulate weld
		9 through 16	IIB	0.50	2.00	4.25	Air cooled from 1700° F to simulate weld
		17 through 36	IIB	2.90	4.90	10.40	As received
A517 grade H	HS	1 through 11	IIA	2.15	4.93	10.25	As received
	HH	1 through 8	IIB	0.75	2.00	4.25	As received
A514 type J	JN	1 through 11	IIA	0.90	4.93	10.25	As received
	JJ	1 through 18	IIB	0.90	4.90	10.40	As received
A572 grade 50	DN	1 through 11	IIA	0.90	4.93	10.25	As received
A572 grade 60	EN	1 through 11	IIA	0.90	4.93	10.25	As received
A588 grade A	ID	1 through 11	IIA	2.90	4.93	10.25	As received
	II	1 through 8	IIB	2.90	4.90	10.40	As received
AISI 1040	GN	1 through 11	IIA	0.90	4.93	10.25	Austenitized 1550°F, water quenched, tempered at 1225°F
AISI 1035[b]	U16N	0 through 19	IIB	1.46	4.90	10.40	As fabricated
	U14S	0	IIB	1.46	4.90	10.40	As fabricated
	U14N	0	IIB	1.46	4.90	10.40	As fabricated

[a]See figure 3.

[b]Material removed from eyebar members of West Carquinez Bridge, see figures 1 and 2.

Table 9.—Field Test Sites

Sites	Reason for selection	Site contact
West Span, Snohomish River Bridge, State Route 529, Everett, Washington	Proximity to pulp mill emitting sulfur compounds	L. L. Waite District Bridge Maintenance Engineer Washington State Dept. of Highways 10833 Northrop Way NE Bellevue, Washington 98004 Phone (206) 822-8403 Walt Zandecki, Bridge Foreman
Hood Canal Floating Bridge, Washington State	Sea water environment. Reported stress corrosion cracking of cable wire	D. D. Ernst District Maintenance Engineer Washington State Dept. of Highways P.O. Box 327 Olympia, Washington 98504 Gene Wisnant, Bridge Foreman Phone (206) 779-337
Huey Long Memorial Bridge, U.S. 190, Mississippi River, Baton Rouge, Louisiana	Proximity to chemical plants, oil refiners, and aluminum smelter	Davis S. Huval Bridge Design Engineer Louisiana Dept. of Highways P.O. Box 44245, Capitol Station Baton Rouge, Louisiana 70804 Attention: James C. Porter Assistant Bridge Design Engineer Phone (504) 389-5310
Silver Memorial Bridge, West Virginia Highway Bridge No. 2765 Henderson, West Virginia	Proximity to site where the Point Pleasant Bridge collapsed in 1967 due to stress corrosion cracking of an eyebar	Garland W. Steele Director Materials Control, Soil and Testing Division 312 Michigan Avenue Charleston, West Virginia 25311 Attention: H. Bert Hood, Jr. Phone (304) 348-3193
Franklin Institute Science Museum, Philadelphia, Pennsylvania	Reported high levels of sulfur dioxide Proximity to continuous air monitoring station from which records of atmosphere conditions are available	James Harrington Director of Exhibits, Franklin Institute Benjamin Franklin Park Way Philadelphia, Pa 19103 Lynn Perkins Assistant Director Exhibits Phone (215) 448-1192
West Carquinez Highway Bridge, Vallejo, California	Eyebar member corrosion problems	Charles Seim, Chief Operation Support Branch Toll Bridges, P.O. Box 3366, Rincon Annex San Francisco, CA 94119 Phone (415) 464-0776 Robert McDougald Bridge Manager, Toll Plaza Carquinez Bridge Phone (707) 644-4036

Table 10.– Analysis of West Carquinez Bridge Corrosion Product Samples

Analysis method	Sample	Compound identification	Elements		
			Major amounts	Minor amounts	Trace amounts
X-ray spectrography	East truss, as received		Fe	Mn, Si, P, S, Ca, Pb, K	Cl
X-ray spectrography	East truss, H_2O extract	$Ca(SO_4) \cdot \frac{1}{2} H_2O$ and lesser amounts of NaCl	Ca, Cl, S, Si, Mn	Fe, Pb, K, P	Br, Cd, Ba
X-ray spectrography	West truss, H_2O extract	Same as east truss sample	Same as east truss sample	Same as east truss sample	Br, Sr, Cd, Ba
Infrared spectrography	East truss, solvent extract	Aliphatic hydrocrabon mixed with aromatic component			
Infrared spectrography	West truss, solvent extract	Same as east truss sample			
Infrared spectrography	East truss, H_2O extract	Sulfate or silicate compound			
Infrared spectrography	West truss, H_2O extract	Same as east truss sample			

Table 11.—Industries Within an Approximate 5 Mile Radius of Carquinez Bridge (ref. 13)

Company	Description of products
California and Hawaiian Sugar Company (Located east of bridge)	Sugar refinery.
Virginia Chemical Company (Located west of bridge)	Production of industrial chemicals. Also, site of lead smelter that operated during the life of the bridge and closed about 1970.
Union Oil Company of America (Located southwest of bridge)	Petroleum products.
Hercules, Incorporated (Located southwest of bridge)	Ammonia, nitric acid, nitrogen textroxide, nitrate of ammonia, and urea.
Sequoia Refining Corporation (Located southwest of bridge)	Petroleum refining.
Collier Carbon and Chemical Company (Located south of bridge)	Petroleum coke to calcined coke.

Table 12.—Results of DCB Stress Corrosion Test in Sulfur Dioxide

Environment	Steel	Specimen number[a]	Stress intensity, ksi-in$^{1/2}$		Exposure time, hr	Remarks
			Initial	Final		
[b]Continuous flow of aqueous solution saturated with SO_2	A36	AD5	43.5	43.5	504	No SCC
		AD6	43.5	43.5	504	
		AD10	21.0	21.0	504	
	A441	CD5	70.5	70.5	543	
		CD6	57.5	57.5	543	
		CD10	30.5	30.5	543	
	AISI 1040	GN5	36.0	36.0	503	
		GN6	27.0	27.0	503	
		GN10	14.5	14.5	503	
[c]Periodic exposure to aqueous solution saturated with SO_2	AISI 1035	U16N16	42.9	42.9	9000	
		U16N17	61.3	61.3	9000	
Stagnant solution saturated with SO_2	A588 grade A	II3	61.3	61.3	1416	
		II4	48.1	48.1	1416	
	A514 type E	BB3	71.2	71.2	1200	
		BB4	57.2	57.2	1200	
	A514 type F	FF19	105.0	105.0	1056	
		FF20	60.3	60.3	1200	
	A517 grade H	HH3	39.7	39.7	1200	
		HH4	37.0	37.0	1200	
	A514 type J	JJ3	129.1	129.1	1416	
		JJ4	78.4	78.4	1416	
[c]Periodic exposure to 50 ppm SO_2 aqueous solution	A588 grade A	II5	60.6	60.6	13 488	
		II6	58.6	58.6	13 488	
	A441, water quenched[d]	CC3	70.1	70.1	13 300	
		CC4	47.8	47.8	13 300	
	A514 type F, water quenched[d]	FF3	104.2	104.2	13 300	
		FF4	53.7	53.7	13 300	
	A514 type F, air cooled[e]	FF11	83.8	83.8	13 300	
		FF12	41.0	41.0	13 300	
	A514 type F, as-received	FF21	109.0	109.0	13 176	
		FF22	68.8	68.8	13 176	
	A517 grade H	HH5	42.4	42.4	13 000	
		HH6	32.1	32.1	13 000	
	A514 Type J	JJ5	125.0	125.0	13 538	
		JJ6	60.2	60.2	13 538	
	A514 Type E	BB5	81.4	81.4	13 300	
		BB6	51.7	51.7	13 300	
	AISI 1035	U16N4	40.2	40.2	9 000	
		U16N7	43.8	43.8	9 000	No SCC

[a]See table 8 for specimen dimensions.

[b]Test initiated in phase IIA (ref. 3)

[c]Test solution applied to crack tip twice daily

[d]Water quenched from 1700° F to simulate weld structure

[e]Air cooled from 1700° F to simulate weld structure

Table 13.—Results of DCB Stress Corrosion Test in Hydrogen Sulfide

Environment	Steel	Specimen number[a]	Stress intensity, ksi-in$^{1/2}$		Exposure time, hr	Remarks
			Initial	Final		
Continuous flow of 3.5% NaCl and 0.5% acetic acid solution saturated with H_2S[b]	A36	AD7	44.5	44.5	840	No SCC
		AD8	33.5	33.5	840	No SCC
		AD11	21.0	21.0	840	No SCC
	A441	CD7	74.0	74.0	816	No SCC
		CD8	57.5	57.5	816	No SCC
		CD11	29.5	29.5	816	No SCC
	A588 grade A	ID7	68.0	68.0	816	No SCC
		ID8	53.0	53.0	816	No SCC
		ID11	27.5	27.5	816	No SCC
	A572 grade 60	EN11	22.5	22.5	1 000	No SCC
		EN10	46.0	46.0	1 000	No SCC
		EN9	57.5	57.5	1 000	No SCC
	A514 type E	BD7	50.0	45.0	772	0.28 crack growth
		BD10	33.0	33.0	772	No SCC
		BD11	17.0	17.0	772	No SCC
	A514 type F	FD7	59.0	59.0	768	No SCC
		FD8	39.0	39.0	768	No SCC
		FD11	19.0	19.0	768	No SCC
	A517 grade H	HS7	42.5	36.0	820	0.38 crack growth
		HS8	30.0	30.0	820	No SCC
		HS11	16.0	16.0	820	No SCC
	A514 type J	JN11	61.0	–	408	Growth out of plane
		JN10	39.0	35.5	835	0.22 crack growth
		JN9	20.0	18.5	835	0.14 crack growth
	AISI 1040	GN7	37.5	37.5	840	No SCC
		GN8	26.0	26.0	840	No SCC
		GN11	14.0	14.0	840	No SCC
	A441, 5% cold worked	CCW6A	37.0	37.0	764	No SCC
		CCW6B	18.5	18.5	764	No SCC
	A514 type F, 5% cold worked	FCW6A	40	40	764	No SCC
		FCW6B	19.5	19.5	764	No SCC
Periodic exposure to 3.5% NaCl and 0.5% acetic acid solution saturated with H_2S[c]	A514 type F, as received	FF23	56.9	56.9	13 320	No SCC
		FF24	36.5	36.5	13 320	No SCC
	AISI 1035	U16N14	49.0	49.0	9 000	No SCC
		U16N15	49.8	49.8	9 000	No SCC
Stagnant 3.5% NaCl and 0.5% acetic acid solution saturated with H_2S	A588 grade A	II7	62.3	62.3	1 416	No SCC
		II8	51.9	51.9	1 416	No SCC
	A517 grade H	HH7	43.9	33.2	1 200	0.31 crack growth
		HH8	37.0	23.8	1 200	0.51 crack growth
Periodic exposure to 5 ppm Aqueous H_2S solution[c]	A514 type E	BB1	52.4	52.4	13 300	No SCC
		BB2	37.1	37.1	13 300	
	A441, water quenched	CC1	87.7	87.7	13 300	
		CC2	53.1	53.1	13 300	
	A514 type F, water quenched	FF1	45.0	45.0	13 550	
		FF2	33.2	33.2	13 550	
	A514 type F, air cooled	FF9	51.4	51.4	13 300	
		FF10	39.2	39.2	13 300	
	A514 type F, as received	FF17	53.9	53.9	13 344	
		FF18	38.2	38.2	13 344	
	A517 grade H	HH1	42.4	42.4	13 300	
		HH2	35.1	35.1	13 300	
	A588 grade A	II1	50.4	50.4	13 488	
		II2	62.2	62.2	13 488	
	A514 type J	JJ1	40.3	40.3	13 538	
		JJ2	24.0	24.0	13 538	
	AISI 1035	U16N8	39.2	39.2	9 000	
		U16N9	47.9	47.9	9 000	No SCC

[a]See table 8 for specimen dimensions

[b]Test initiated in phase IIA (ref. 3)

[c]Test solution applied to crack tip twice daily

Table 14.—Results of DCB Stress Corrosion Test in Calcium Nitrate and Ammonium Nitrate

Environment	Steel	Specimen number[a]	Stress intensity, ksi-in$^{1/2}$		Exposure time, hr	Remarks
			Initial	Final		
Continuous flow of 60% $Ca(NO_3)_2$ and 3% NH_4NO_3 aqueous solution[b]	A36	AD3	45.0	45.0	8 600	No SCC
		AD4	31.2	31.2		
	A441	CD3	74.5	74.5		
		CD4	54.0	54.0		
	A514 type E	BD3	74.5	74.5		
		BD4	49.0	49.0		
	A514 type F	FD3	106.0	106.0		
		FD4	117.0	117.0		
	A517 grade H	HS3	39.5	39.5		
		HS6	31.0	31.0		
	A514 type J	JN4	117.0	117.0		
		JN5	64.5	64.5		
	A572 grade 50	DN3	63.0	63.0		
		DN4	49.7	49.7		
	A572 grade 60	EN3	49.0	49.0		
		EN4	60.0	60.0		
	A588 grade A	ID3	68.5	68.5		
		ID4	53.0	53.0		
	AISI 1040	GN1	37.5	37.5		
		GN4	25.5	25.5		
	A441, 5% cold worked	CCW4A	36.0	36.0		
		CCW4B	19.5	19.5		
	A514 type F, 5% cold worked	FCW2A	72.8	72.8		
		FCW2B	28.8	72.8	8 600	
Periodic exposure to 60% $Ca(NO_3)_2$ and 3% NH_4NO_3 aqueous solution[c]	AISI 1035	U16N18	41.0	41.0	9 000	
		U16N19	51.0	51.0	9 000	
		U16NO	41.2	41.2	8 784	
		U14NO	46.7	46.7	8 784	No SCC
Periodic exposure to 5% $Ca(NO_3)_2$ and 0.25% NH_4NO_3 aqueous solution[c]	A441, water quenched	CC5	101.0	43.2	13 300	1.13 in. crack growth
		CC6	44.8	28.0	13 300	0.60 in. crack growth
	A514 type F, water quenched	FF5	94.0	(d)	13 300	SCC[d]
		FF6	50.5	(d)	13 300	SCC[d]
	A514 type F, air cooled	FF13	79.1	(d)	13 300	SCC[d]
		FF14	40.1	40.1	13 300	No SCC
	AISI 1035	U16N10	45.8	45.8	9 000	No SCC
		U16N11	42.9	42.9	9 000	No SCC

[a]See table 8 for specimen dimensions

[b]Test initiated in phase IIA

[c]Test solution applied to crack tip twice daily

[d]Crack branching out of plane makes final stress intensity calculation invalid

Table 15.—Results of DCB Stress Corrosion Test in 3.5% Sodium Chloride Aqueous Solution

Environment	Steel	Specimen number[a]	Stress intensity, ksi-in.$^{1/2}$		Exposure time, hr	Remarks
			Initial	Final		
Continuous flow of 3.5% NaCl aqueous solution[b]	A36	AD3	45.0	45.0	8 600	No SCC
		AD4	31.2	31.2		
	A441	CD3	74.5	74.5		
		CD4	54.0	54.0		
	A514 type E	BD3	74.5	74.5		
		BD4	49.0	49.0		
	A514 type F	FD3	106.0	106.0		
		FD4	117.0	117.0		
	A517 grade H	HS3	39.5	39.5		
		HS6	31.0	31.0		
	A514 type J	JN4	117.0	117.0		
		JN5	64.5	64.5		
	A572 grade 50	DN3	63.0	63.0		
		DN4	49.7	49.7		
	A572 grade 60	EN3	49.0	49.0		
		EN4	60.0	60.0		
	A588 grade A	ID3	68.5	68.5		
		ID4	53.0	53.0		
	AISI 1040	GN1	37.5	37.5		
		GN4	25.5	25.5		
	A441, 5% cold worked	CCW4A	36.0	36.0		
		CCW4B	19.5	19.5		
	A514 type F, 5% cold worked	FCW2A	72.8	72.8		
		FCW2B	28.8	28.8	8 600	
Periodic exposure to 3.5% NaCl aqueous solution[c]	A441, water quenched	CC7	77.0	77.0	13 300	
		CC8	48.3	48.3	13 300	
	A514 type F, air cooled	FF15	76.2	76.2	13 300	
		FF16	42.5	42.5	13 300	
	AISI 1035	U16N12	47.3	47.3	9 000	
		U16N13	45.6	45.6	9 000	No SCC

[a]See table 8 for specimen dimensions

[b]Test initiated in phase IIA (ref. 3)

[c]Test solution applied to crack tip twice daily

Table 16.—Results of DCB Stress Corrosion Test in 0.26% Calcium Sulfate Aqueous Solution

Environment	Steel	Specimen number[a]	Stress intensity, ksi-in$^{1/2}$		Exposure time, hr	Remarks
			Initial	Final		
Periodic exposure to 0.26% $Ca(SO_4)$ aqueous solution[b]	AISI 1035	U16N2	39.8	39.8	8 784	No SCC
		U16N3	41.2	41.2	8 784	No SCC
		U16N1	42.4	42.4	8 784	No SCC
		U14SO	40.1	40.1	8 784	No SCC

[a]See table 8 for specimen dimensions

[b]Test solution applied to crack tip twice daily

Table 17.—Summary of Alloys Susceptible to Stress Corrosion

Alloy	Condition	K_{ISCC}, ksi-in$^{1/2}$	Environment
A514 type E	As received	45	3.5% NaCl/0.5% acetic acid solution saturated with H_2S
A514 type J[a]	As received	18	
A517 grade H	As received	[b]36	
	As received	[c]24	
A441	Water quenched	28	5% $Ca(NO_3)_2$/0.25% NH_4NO_3 aqueous solution
A514 type F	Water quenched	<50	
A514 type F	Air cooled	<79>40	

[a]Reported fully in reference 3.

[b]Continuous flow of solution

[c]Stagnant solution

Table 18.—Description of DCB Specimens Remaining at Test Sites

Test site	Placement date	Steel	Specimen identification[a]	Deflection, in.	Initial crack length,[b] in.	Initial stress intensity, ksi-in$^{1/2}$	Exposure time at 10-31-76, hr
Franklin Institute Philadelphia, Pennysylvania	7-31-75	A36 A514 E A514 F A514 J	AA6 BB12 FF30 JJ12	0.0195 0.0300 0.0645 0.0635	3.06 1.31 3.12 3.02	40 91 128 133	10 992
West Carquinez Highway Bridge Vallejo, California	9-11-75	A36 A514 E A514 F A514 J AISI 1035	AA12 BB18 FF36 JJ18 U16N6	0.0200 0.0295 0.0605 0.0640 0.0270	3.05 1.32 3.06 3.01 3.11	41 88 124 134 54	9 984
U. S. 190 Mississippi River Bridge Baton Rouge, Louisiana	7-28-75	A36 A514 E A514 F A514 J	AA8 BB14 FF32 JJ14	0.0200 0.0295 0.0660 0.0645	3.04 1.32 3.41 3.09	41 88 118 131	11 064
Silver Memorial Bridge Henderson, West Virginia	7-30-75	A36 A514 E A514 F A514 J	AA10 BB16 FF34 JJ16	0.0195 0.0295 0.0655 0.0640	3.02 1.37 3.07 3.05	41 90 133 132	11 016
West Span, Snohomish River Bridge State Route 529 Everett, Washington	6-16-75	A36 A514 E A514 F A514 J	AA2 BB8 FF26 JJ8	0.0205 0.0310 0.0615 0.0640	3.04 1.32 3.07 2.97	42 92 125 137	12 072
Hood Canal Floating Bridge Washington State	6-18-75	A36 A514 E A514 F A514 J	AA3 BB10 FF27 JJ10	0.0200 0.0300 0.0635 0.0640	3.01 1.31 3.04 2.91	42 91 131 140	12 024

[a]Total deflection of the two arms of DCB specimen at the load point

[b]Measured along the sides of the specimen

Table 19.—Results of Field Testing Double Cantilever Beam Stress Corrosion Specimens

Test site location	Steel	Specimen identification	Stress intensity, ksi-in$^{1/2}$	Exposure time, hr	Remarks
West Span, Snohomish River Bridge, State Route 529 Everett, Washington	A514 F	FF25	[a]205	9 750	No SCC
	A514 E	BB7	87.2		
	A514 J	JJ7	162.9		
	A36	AA1	41.4		
Hood Canal Floating Bridge Washington State	A514 F	FF28	119.3	10 080	No SCC
	A514 E	BB9	76.9		
	A514 J	JJ9	131.2		
	A36	AA4	40.4		
West Carquinez Bridge, Vallejo, California	AISI 1035	U16N5	48.6	8 790	No SCC
	A514 F	FF35	137.3		
	A514 E	BB17	75.6		
	A514 J	JJ17	131.2		
	A36	AA11	41.2		
Franklin Institute, Philadelphia, Pennsylvania	A514 F	FF29	117.8	8 900	No SCC
	A514 E	BB11	87.6		
	A514 J	JJ11	128.1		
	A36	AA5	45.8		
U.S. 190, Mississippi River Bridge, Baton Rouge, Louisiana	A514 F	FF31	133.9	8 930	No SCC
	A514 E	BB13	76.2		
	A514 J	JJ13	131.2		
	A36	AA7	40.9		
Silver Memorial Bridge, Henderson, West Virginia	A514 F	FF33	114.2	8 900	No SCC
	A514 E	BB15	79.7		
	A514 J	JJ15	126.6		
	A36	AA9	39.9		

[a]Not valid—yield strength of specimen exceeded

Table 20.—Results of Bolt Stress Corrosion Test in Sulfur Dioxide

Environment	Bolt type	Finish	Specimen identification	Load, kip	Exposure time, hr	Remarks
[a]Solution saturated with SO_2	3/4 10 UNC ASTM A490	Bare	B61 B62	30 29	1 272 1 272	No SCC
		Mechanically galvanized	M61 M62	37 30	1 560 1 560	
	7/8 9 UNC ASTM A325	Bare	B71 B72	47 47	1 272 1 272	
		Hot dip galvanized	G71 G72	47 44	1 272 1 272	
		Mechanically galvanized	M71 M72	46 47	1 560 1 560	
	1-1/8 7 UNC ASTM A325	Bare	B91 B92	57 60	840 840	
		Hot dip galvanized	G91 G92	60 61	840 840	
[b]Solution 50 ppm SO_2	3/4 10 UNC	Bare	B67 B68	32 29	11 750 11 750	
		Mechanically galvanized	M611 M612	38 41	7 176 7 176	
	7/8 9 UNC	Bare	B77 B78	47 45	11 750 11 750	
		Hot dip galvanized	G711 G712	49 49	8 256 8 256	
		Mechanically galvanized	M711 M712	43 48	8 256 8 256	
	1-1/8 9 UNC	Bare	B911 B912	63 62	8 256 8 256	
		Hot dip galvanized	G911 G912	78 60	7 500 7 500	No SCC

[a]Stagnant aqueous solution saturated with SO_2

[b]Stagnant aqueous solution containing 50 ppm SO_2

Table 21.—Results of Bolt Stress Corrosion Test in Hydrogen Sulfide

Environment	Bolt type	Finish	Specimen identification	Load, kip	Exposure time, hr	Remarks
[a]Solution saturated with H_2S	3/4 10 UNC ASTM A490	Bare	B63	34	1 008	No SCC
			B64	33	72	Shank failure
		Mechanically galvanized	M63	33	480	Head-to-shank failure
			M64	33	552	Head-to-shank failure
	7/8 9 UNC ASTM A325	Bare	B73	47	1 008	No SCC
			B74	44	672	Thread root failure
		Hot dip galvanized	G73	47	552	Shank failure
			G74	46	240	Thread root failure
		Mechanically galvanized	M73	63	1 560	No SCC
			M74	39	1 560	No SCC
	1-1/8 7 UNC ASTM A325	Bare	B93	57	744	Thread root failure
			B94	61	[b]<1 008	Thread root failure
		Hot dip galvanized	G93	59	[b]<1 008	Thread root failure
			G94	61	936	Thread root failure
[c]Solution containing 5 ppm H_2S	3/4 10 UNC ASTM A490	Bare	B65	33	11 750	No SCC
			B66	33	11 750	
		Mechanically galvanized	M69	32	8 256	
			M610	41	8 256	
	7/8 9 UNC ASTM A325	Bare	B75	43	11 750	
			B76	46	11 750	
		Hot dip galvanized	G79	43	11 750	
			G710	47	11 750	
		Mechanically galvanized	M79	47	8 256	
			M710	43	8 256	
	1-1/8 7 UNC ASTM A325	Bare	B99	61	8 256	
			B910	68	8 256	
		Hot dip galvanized	G99	67	7 500	
			G910	92	7 500	No SCC

[a]Stagnant 3.5% NaCl/0.5% acetic acid solution saturated with H_2S

[b]When bolt was torqued after removal from test, through crack was discovered

[c]Stagnant aqeuous solution containing 5 ppm H_2S

Table 22.—Results of Bolt Stress Corrosion Test in Calcium Nitrate/Ammonium Nitrate Solutions

Environment	Bolt type	Finish	Specimen identification	Load, kip	Exposure time, hr	Remarks
[a]60% $Ca(NO_3)_2$ /3% NH_4NO_3 Solution	3/4 10 UNC ASTM A490	Mechanically galvanized	M65 M66	34 36	8 256 8 256	No SCC
	7/8 9 UNC ASTM A325	Hot dip galvanized	G75 G76	44 44	9 500 9 500	
		Mechanically galvanized	M75 M76	52 50	8 736 8 736	
	1-1/8 7 UNC ASTM A325	Bare	B95 B96	61 60	9 500 9 500	
		Hot dip galvanized	G95 G96	63 62	9 500 9 500	
[b]5% $Ca(NO_3)_2$/ 0.25% NH_4NO_3 solution	3/4 10 UNC ASTM A490	Bare	B69 B610	36 41	8 256 8 256	
		Mechanically galvanized	M613	34	8 256	
	7/8 9 UNC ASTM A325	Bare	B79 B710	44 46	9 500 9 500	
		Hot dip galvanized	G713 G714	48 46	8 256 8 256	
		Mechanically galvanized	B713	43	8 256	
	1-1/8 7 UNC ASTM A325	Bare	B913 B914	64 64	8 256 7 500	
		Hot dip galvanized	G913 G914	60 62	7 500 7 500	No SCC

[a]Stagnant aqueous solution containing 60% $Ca(NO_3)_2$ and 3% NH_4NO_3

[b]Stagnant aqueous solution containing 5% $Ca(NO_3)_2$ and 0.25% NH_4NO_3

Table 23.—Results of Bolt Stress Corrosion Test in 3.5% Sodium Chloride Solution

Environment	Bolt type	Finish	Specimen identification	Load, kip	Exposure time, hr	Remarks
3.5% NaCl solution[a]	3/4 10 UNC ASTM A490	Mechanically galvanized	M67 M68	32 41	8 256 8 256	No SCC
	7/8 9 UNC ASTM A325	Hot dip galvanized	G77 G78	46 43	9 650 9 650	
		Mechanically galvanized	M77 M78	48 43	8 736 8 736	
	1-1/8 7 UNC ASTM A325	Bare	B97 B98	69 78	8 256 8 256	
		Hot dip galvanized	G97 G98	62 67	7 500 7 500	No SCC

[a]Stagnant aqueous solution containing 3.5% NaCl

Table 24.—Results of Wire Stress Corrosion Test in 50 ppm Sulfur Dioxide Aqueous Solution

Wire materials	Specimen identification	Notch depth, in.	Root radius, in.	Applied stress, ksi	% TUS[a]	Exposure time, hr	Remarks
Bare suspension wire, 0.188 in. diameter	B1	0.020	0.001	97	39	10 180	No failure
	B4	0.013	0.004	124	50	8 860	
	B7	0.021	0.002	97	39	8 860	
	B10	0.020	0.002	124	50	7 060	
Dip galvanized suspension wire, 0.192 in. diameter	C1	0.015	0.004	83	38	10 180	
	C4	0.015	0.003	110	50	8 860	
	C7	0.020	0.003	97	44	8 860	
	C10	0.022	0.003	124	57	7 060	
Electrogalvanized suspension wire, 0.187 in. diameter	E1	0.016	0.003	83	36	10 180	
	E4	0.017	0.006	110	48	8 860	
	E7	0.020	0.005	97	42	8 860	
	E10	0.021	0.008	124	54	7 060	
Bare prestressing wire, 0.128 in. diameter	PB1	0.012	0.003	207	78	9 388	
	PB4	0.012	0.002	221	83	8 860	
	PB7	0.012	0.002	221	83	7 060	
	PB10	0.012	0.003	221	83	7 060	
	PB5	0.011	0.003	180	67	6 720	
Galvanized suspension (prototype) wire, 0.108 in. diameter	DC1	0.011	0.002	124	63	7 060	
	DC4	0.011	0.002	124	63	7 060	
	DC7	0.011	0.002	124	63	7 060	
	DC10	0.013	0.002	124	63	7 060	No failure

[a]Applied load as a percent of tensile ultimate strength

Table 25.—Results of Wire Stress Corrosion Test in 5 ppm Hydrogen Sulfide Aqueous Solution

Wire materials	Specimen identification	Notch depth, in.	Root radius, in.	Applied stress, ksi	% TUS[a]	Exposure time, hr	Remarks
Bare suspension wire, 0.188 in. diameter	B2	0.022	0.002	97	39	10 180	No failure
	B5	0.024	0.003	124	50	8 860	
	B8	0.021	0.003	97	39	8 860	
	B11	0.019	–	124	50	7 060	
Dip galvanized suspension wire, 0.192 in. diameter	C2	0.021	0.003	83	38	10 180	
	C5	0.018	0.003	110	50	8 860	
	C8	0.021	0.003	97	44	8 860	
	C11	0.020	0.004	124	57	7 060	
Electrogalvanized suspension wire, 0.187 in. diameter	E2	0.018	0.004	83	36	10 180	
	E5	0.019	0.007	110	48	8 860	
	E8	0.019	0.006	124	42	7 060	
	E11	0.020	0.004	124	54	7 060	
Bare prestressing wire, 0.128 in. diameter	PB2	0.012	0.002	207	78	9 388	
	PB16	0.011	0.003	221	83	8 860	
	PB11	0.011	0.003	180	67	6 720	
Galvanized suspension (prototype) wire, 0.108 in. diameter	DC5	0.010	0.002	124	63	7 060	
	DC8	0.012	0.002	124	63	7 060	
	DC11	0.014	0.002	124	63	7 060	No failure

[a]Applied load as a percent of tensile ultimate strength

Table 26.—Results of Wire Stress Corrosion Test in 5% Calcium Nitrate/0.25% Ammonium Nitrate Aqueous Solution

Wire materials	Specimen identification	Notch depth, in.	Root radius, in.	Applied stress, ksi	% TUS[a]	Exposure time, hr	Remarks
Bare suspension wire, 0.188 in. diameter	B3	0.021	0.001	97	39	10 180	
	B6	0.016	–	124	50	8 860	No failure
	B9	0.022	0.003	124	50	7 060	
	B12	0.022	0.002	124	50	7 060	
Dip galvanized suspension wire, 0.192 in. diameter	C3	0.019	0.004	83	38	10 180	
	C6	0.020	0.003	110	50	8 860	No failure
	C9	0.021	0.003	124	57	7 060	
	C12	0.020	0.003	124	57	7 060	
Electrogalvanized suspension wire, 0.187 in. diameter	E3	0.016	0.005	83	36	10 160	
	E6	0.018	0.004	110	48	8 860	No failure
	E9	0.018	0.006	124	54	7 060	
	E12	0.020	0.005	124	54	7 060	
Bare prestressing wire, 0.128 in. diameter	PB3	0.011	0.002	207	78	2 450	Failed
	PB6	0.010	0.001	221	83	2 800	Failed
	PB9	0.012	0.002	221	83	7 060	No Failure
	PB12	0.011	0.003	221	83	7 060	No Failure
	PB8	0.012	0.002	150	56	4 580	Failed
	PB13	0.012	0.004	180	67	3 770	Failed
Galvinized suspension (prototype) wire, 0.108 in. diameter	DC3	0.014	0.002	124	63	7 060	
	DC6	0.014	0.002	124	63	7 060	No failure
	DC9	0.013	0.002	124	63	7 060	
	DC12	0.012	0.002	124	63	7 060	

[a]Applied load as a percent of tensile ultimate strength.

REFERENCES

1. *Highway Accident Report: Collapse of U.S. 35 Highway Bridge, Point Pleasant, West Virginia, December 15, 1967,* report NTSB-HAR-71-1, National Transport Safety Board, 1971.

2. Carter, C. S., Hyatt, M. V., and Cotton, J. E., *Stress Corrosion Susceptibility of Highway Bridge Construction Steels, Phase I,* Boeing Company report D6-60159-2 to Federal Highway Administration, April 1972.

3. Carter, C. S., and Caton, R. G., *Stress Corrosion Susceptibility of Highway Bridge Construction Steels, Phase IIA,* Boeing Company report D6-60217 to Federal Highway Administration, April 1973.

4. Letter to R. G. Caton dated June 17, 1975 from Eric F. Mordlin, Chief, Sructural Materials Branch, Transportation Laboratory, California Department of Transportation.

5. Letter to Jim Guthrie dated May 19, 1975 from D. M. Maze, Plating Systems Department, Mechanical Plating, 3M Company, Saint Paul, Minnesota 55101.

6. Brown, B. F., "The Application of Fracture Mechanics to Stress Corrosion Testing" *Metallurgical Review 13, Metals and Materials,* vol 2, 1968, p 171.

7. Smith, H. R., and Piper, D. E., "Stress Corrosion Testing With Precracked Specimens," in *Stress Corrosion Cracking in High Strength Steels and in Titanium and Aluminum Alloys,* B. F. Brown, ed., Naval Research Laboratory, 1972.

8. Mostovoy, S., Crosley, P. B., and Ripling, E. J., "Use of Crack Line Loaded Specimens for Measuring Plane Strain Fracture Toughness," *J. Matls.*, vol 2, no. 3, 1967, p 661.

9. Speidel, M. O., and Hyatt, M. V., "Stress Corrosion Cracking of High Strength Aluminum Alloys" in *Advances in Corrosion Science and Technology,* M. G. Fontana and R. W. Staehle, eds., Plenum Press, 1972.

10. Hoagland, R. G., Rosenfield, A. R., and Hahn, G. T., "Mechanism of Fast Fracture and Arrest in Steels" *Met. Trans.* vol 3, 1972, p 123.

11. Gross, B., and Srawley, J. E., "Stress Intensity Factors by Boundary Collocation for Single Edge Notch Specimens Subject to Splitting Forces," NASA technical note NASA-TN-D-3295, 1966.

12. Hahn, G. T., Sarrate, M., and Rosenfield, A. R., "Plastic Zones in Fe-3 Si Steel Double Cantilever Beam Specimens," *Int. J. Fract. Mech.* vol 7, 1971, p 435.

13. Letter to Reginald G. Caton dated June 3, 1975 from Charles Seim, Chief, Engineering Branch, Toll Bridges, California Department of Transportation.

14. Letter to R. G. Caton dated September 11, 1976 from C. Seim, Chief, Operations Support Branch, Toll Bridges, California Department of Transportation.

15. Everling, W. D., "Stress Corrosion in High Tensile Wire," *Wire and Wire Products,* vol 30, 1955, p 316.

16. Treadaway, K. W. T., "Corrosion of Prestressed Steel Wire in Concrete," *British Corrosion Journal,* 1971, p 66.

☆U.S. GOVERNMENT PRINTING OFFICE: 1977-240-897/2.34